





Review

Physical and Chemical Features of Hydrogen Combustion and Their Influence on the Characteristics of Gas Turbine Combustion Chambers

Elena Anatolievna Shchepakina ^{1,*} , Ivan Alexandrovich Zubrilin ¹ , Alexey Yurievich Kuznetsov ¹, Konstantin Dmitrievich Tsapenkov ¹, Dmitry Vladimirovich Antonov ² , Pavel Alexandrovich Strizhak ² , Denis Vladimirovich Yakushkin ¹, Alexander Gennadievich Ulitichev ³, Vladimir Alexandrovich Dolinskiy ³ and Mario Hernandez Morales ¹ 

¹ Institute of Engine and Power Plant Engineering, Samara National Research University, 34, Moskovskoye Shosse, Samara 443086, Russia

² Energy Engineering School, National Research Tomsk Polytechnic University, 30, Prospekt Lenina, Tomsk 634050, Russia

³ PJSC "UEC-Kuznetsov", Samara 443080, Russia

* Correspondence: shchepakina@yahoo.com

Abstract: Hydrogen plays a key role in the transition to a carbon-free economy. Substitution of hydrocarbon fuel with hydrogen in gas turbine engines and power plants is an area of growing interest. This review discusses the combustion features of adding hydrogen as well as its influence on the characteristics of gas turbine combustion chambers as compared with methane. The paper presents the studies into pure hydrogen or methane and methane–hydrogen mixtures with various hydrogen contents. Hydrogen combustion shows a smaller ignition delay time and higher laminar flame speed with a shift in its maximum value to a rich mixture, which has a significant effect on the flashback inside the burner premixer, especially at elevated air temperatures. Another feature is an increased temperature of the flame, which can lead to an increased rate of nitrogen oxide formation. However, wider combustion concentration ranges contribute to the stable combustion of hydrogen at temperatures lower than those of methane. Along with this, it has been shown that even at the same adiabatic temperature, more nitrogen oxides are formed in a hydrogen flame than in a methane flame, which indicates another mechanism for NO_x formation in addition to the Zeldovich mechanism. The article also summarizes some of the results of the studies into the effects of hydrogen on thermoacoustic instability, which depends on the inherent nature of pulsations during methane combustion. The presented data will be useful both to engineers who are engaged in solving the problems of designing hydrogen combustion devices and to scientists in this field of study.

Keywords: hydrogen; combustion chamber; emission; gas turbine engines; flame blowout



Citation: Shchepakina, E.A.; Zubrilin, I.A.; Kuznetsov, A.Y.; Tsapenkov, K.D.; Antonov, D.V.; Strizhak, P.A.; Yakushkin, D.V.; Ulitichev, A.G.; Dolinskiy, V.A.; Hernandez Morales, M. Physical and Chemical Features of Hydrogen Combustion and Their Influence on the Characteristics of Gas Turbine Combustion Chambers. *Appl. Sci.* **2023**, *13*, 3754. <https://doi.org/10.3390/app13063754>

Academic Editors: Adrian Irimescu and Matt Oehlschlaeger

Received: 9 December 2022

Revised: 26 January 2023

Accepted: 2 March 2023

Published: 15 March 2023



Copyright: © 2023 by the authors. Licensee MDPI, Basel, Switzerland. This article is an open access article distributed under the terms and conditions of the Creative Commons Attribution (CC BY) license (<https://creativecommons.org/licenses/by/4.0/>).

1. Introduction

The increasing desire to use hydrogen (H₂) as a fuel for heat engines and power plants is associated with the need to switch to carbon-free technologies, which in the long term are intended to solve several problems related to global warming [1,2]. In addition, the use of hydrogen fuel makes it possible to increase the theoretical power limit of gas turbine engines and reduce the dependence of aircraft and industrial plants on fossil fuels.

A detailed analysis of the influence of the composition of gaseous fuel, particularly CO, methane, natural gas, syngas, and hydrogen, on the parameters of the combustion process and the characteristics of gas turbine combustors was presented in the work of Taamallah [3]. The logical structure of the analysis is shown in Figure 1. A change in the composition of the fuel leads to a change in its chemical and physical characteristics that, in turn, have an effect on the flame properties (i.e., flame temperature, ignition delay time,

flame speed) and determine the main characteristics of the combustion chamber (pollutant emission, combustion efficiency, static and dynamic stability, flashback). The purpose of this work is to analyze the literature in the field of hydrogen combustion and the effect of adding hydrogen on the characteristics of combustion chambers in comparison to the widely used hydrocarbon fuel—natural gas.

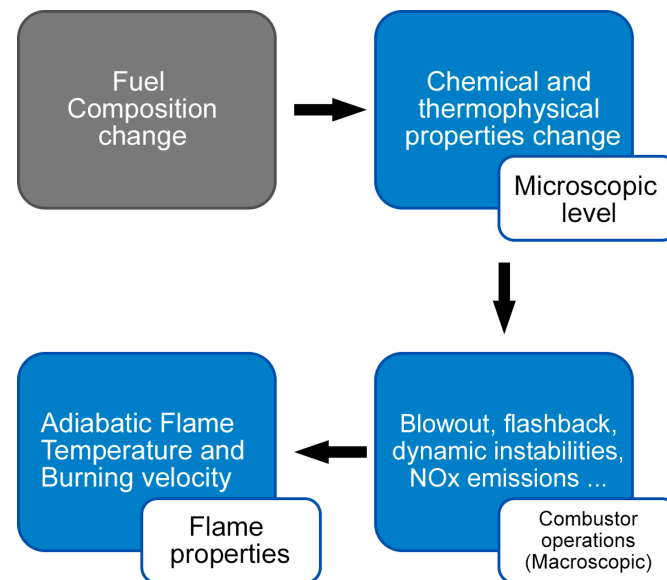


Figure 1. Analysis of fuel composition influence at different levels, adapted from [3].

2. Features of Hydrogen Combustion Processes

2.1. Properties of Hydrogen and Flame Temperature

The use of hydrogen in gas turbine engines and power plants is mainly considered a replacement for widely used natural gas (due to the similarity of their properties, in this paper, natural gas and methane are considered similar fuels). At the first stage of technological re-equipment, partial or complete replacement of natural gas with hydrogen implies no significant construction changes. This possibility can be assessed by comparing the physicochemical properties of hydrogen with the properties of natural gas. The comparison of the physicochemical properties of hydrogen and natural gas is shown in Table 1, where it can be seen that hydrogen has a significantly lower density (about eight times lower than methane), has wider ignition concentration limits, and is generally more reactive than methane. The net calorific value per unit mass is more than three times higher than that for methane, but the volume per unit is nearly half as much. Consequently, for the same thermal power, the required volumetric flow rate of hydrogen is more than twice the flow rate of methane.

Table 1. Properties of hydrogen compared to natural gas [4–7].

	Hydrogen	Natural Gas
Density at 273 K (kg/m ³)	0.09	0.72
Molar mass (kg/kmol)	2.016	16.04
Ignition limits (Φ)	0.1–7.1	0.4–1.6
Low calorific value (MJ/kg)	120	50
Low calorific value (MJ/m ³)	11	36
Maximum laminar flame speed (m/s)	3.25	0.45
Adiabatic flame temperature at Φ = 1 (K)	2402	2216
Stoichiometric coefficient	34.2	17.2
Melting temperature (K)	14	91
Boiling temperature (K)	21	112
Critical temperature (K)	33	191
Critical pressure (amt)	12.8	45.2
Autoignition temperature (K)	850	810

Hydrogen also has a higher adiabatic flame temperature, which can increase the probability of overheating the combustion chamber elements and the turbine while maintaining the excess fuel ratio in the combustion zone. The influence of the content of hydrogen in mixtures with natural gas on the flame temperature is shown in Figure 2. The flame temperature is mainly influenced by a specific heat of combustion and the flame speed. Since the flame temperature and specific heat of combustion are relatively high for hydrogen, during its combustion, while maintaining the stoichiometric coefficient, the flame temperature is higher. It is worth noting that the relative increase in the flame temperature of hydrogen compared to methane is greater for rich mixtures (about +15–17%), slightly less for lean mixtures (+10–12%), and the least of all for stoichiometric mixtures (about 7–8%). Therefore, a rational conclusion is that the heat load on the flame tube head of the combustion chamber can become 10–15% higher when switching to hydrogen fuel, which will require additional efforts to ensure thermal protection. While maintaining the total thermal power of the flame for the combustion chamber, the local thermal power of the flame increases. This is due to the fact that when enriched with hydrogen, the flame becomes more compact.

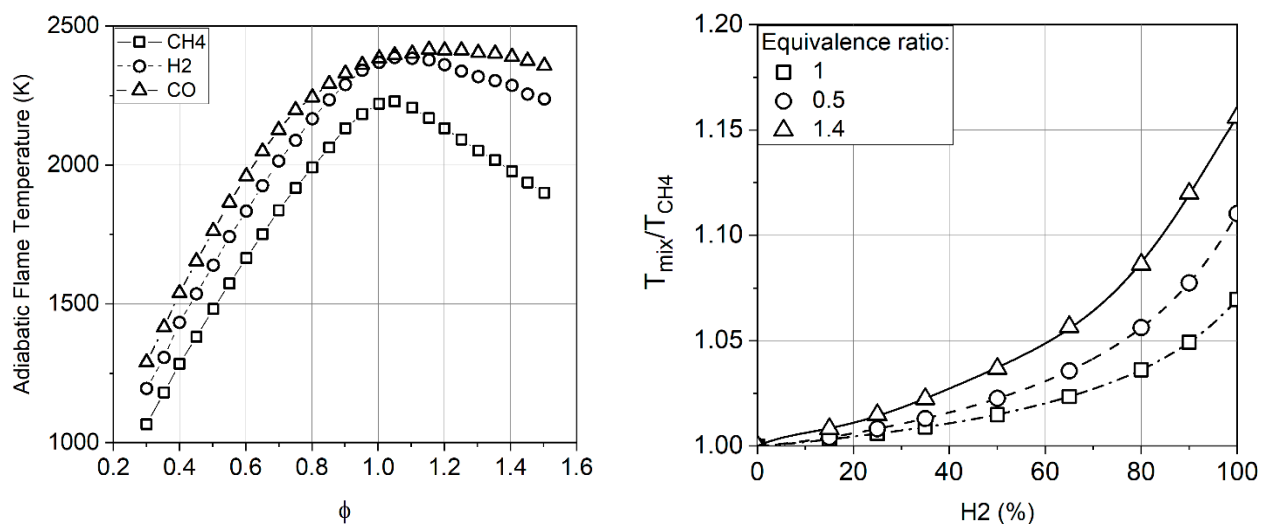


Figure 2. Influence of hydrogen volume concentration on the normalized temperature of the methane–air mixture flame [3,8,9].

2.2. Laminar Flame Propagation Speed

One of the principal properties of a laminar flame is speed propagation. Figure 3 shows the relationship between the laminar flame propagation speed and the equivalence ratio. The first thing worth noting is that the maximum propagation speed of a laminar hydrogen flame is several times higher than the one for methane: 100–120 m/s compared to 30–40 m/s under normal atmospheric conditions. The second feature is the displacement of the maximum laminar flame propagation speed value to the region of rich mixtures. The maximum value of the flame speed of a hydrogen mixture is shifting to the region $\phi = 1.0$ – 1.2 (Figure 3), which approximately corresponds to the position of the maximum of the flame temperature. For combustion chambers, this may mean that rich mixtures will burn more intensively, thus increasing the probability of flashback. However, hydrogen combustion can occur at higher flow velocities without loss of combustion efficiency.

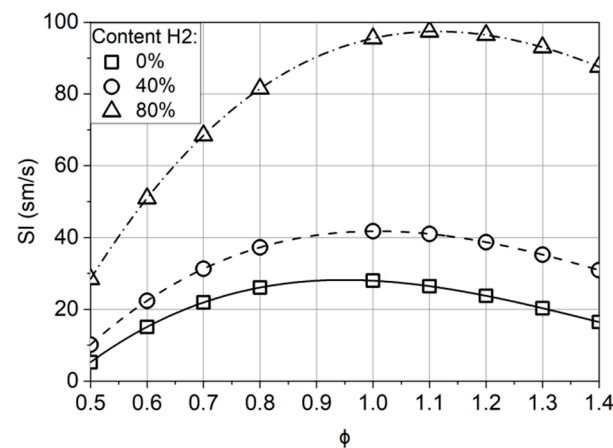


Figure 3. Influence of the molar fraction of hydrogen on the flame propagation speed of a methane–hydrogen mixture at atmospheric pressure and 300 K [9,10].

The effect of pressure on the relative laminar flame speed of methane–hydrogen mixtures is shown in Figure 4.

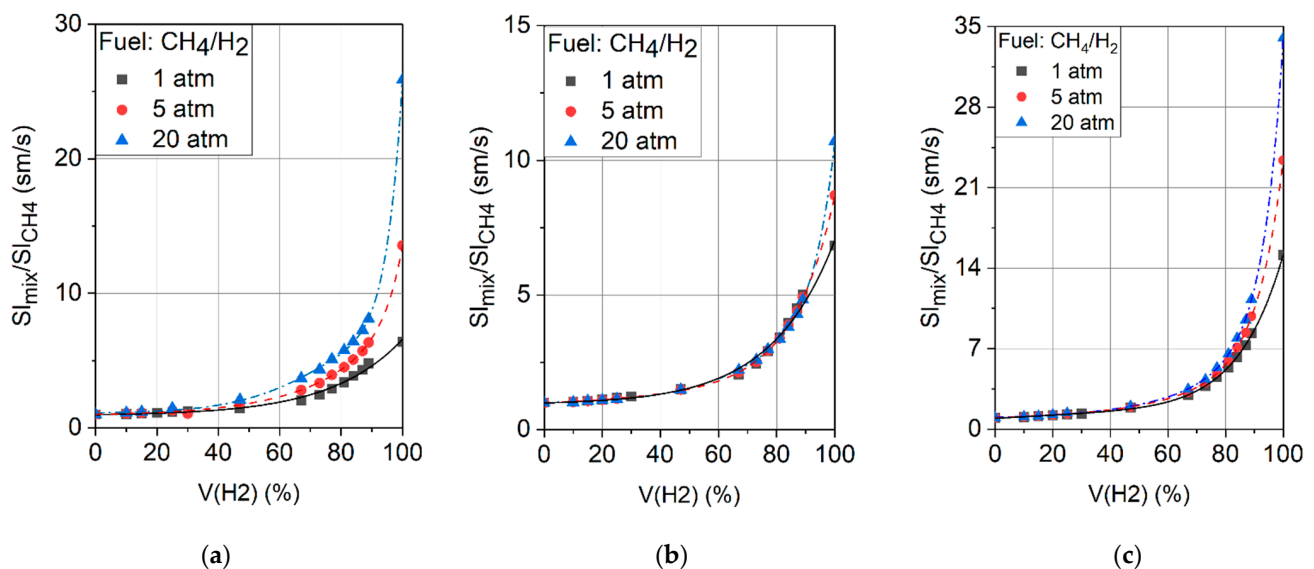


Figure 4. Relationship between the propagation laminar flame speed of methane–hydrogen mixture and the volume concentration of hydrogen [9,11,12] (a) $\phi = 0.6$; (b) $\phi = 1$; (c) $\phi = 1.4$.

The addition of hydrogen has a profound effect on the flame speed of rich mixtures at high pressures (an increase in speed by a factor of ≈ 35 compared to the methane laminar flame speed at the pressure of 20 atm). For lean mixtures, the effect of hydrogen is somewhat smaller compared to rich mixtures, with the increase in the laminar flame of about 25 times. In general, it can be observed that the correlation between the addition of hydrogen and the flame speed largely depends on the pressure and grows as the pressure increases. This complicates the process of extrapolating the results obtained by the atmospheric studies to the real conditions in gas turbine engines, which leads to the need for additional experimental tests for the working process when burning hydrogen in combustion chambers at elevated pressures, thus making the feasibility of such studies much higher than when burning natural gas.

Consequently, a certain pattern can be observed for any composition where an increase in normal flame propagation speed can be divided into three modes: (1) at a hydrogen content of up to 50–60%, an increase in the laminar flame speed with an increase in the proportion of hydrogen is approximately linear and does not exceed 25%, which means

that hydrocarbons predominate in the chemical composition; (2) at the highest levels of hydrogen content (>75–90%), there is an exponential increase in flame speed due to the dominant effect of hydrogen oxidation chemistry, which means that the flame is considered to be predominantly in hydrogen; (3) the range within 60–75% can be considered the area of the parabolic increase in velocity.

2.3. Ignition Delay Time and Autoignition Temperature

One of the most important characteristics of the combustion process is the ignition delay time. In combustion chambers, this value has an effect on the amount of time that is available for pre-mixing the fuel with air before the ignition and combustion (when the air temperature after the compressor is higher than the auto-ignition temperature of the mixture). On the one hand, to achieve a low level of nitrogen oxide emissions, a high-quality fuel–air mixture preparation is required; on the other hand, the premix burner section (premixer) must be designed in such a way as to avoid undesirable ignition within it. Due to the high temperature and pressure at the inlet to the combustion chambers of gas turbines, this becomes a difficult task, and for highly reactive fuels such as hydrogen, it is even more difficult.

Figures 5 and 6 show that the ignition delay time strongly depends on the temperature and composition of the fuel–air mixtures: the ignition delay time decreases by orders of magnitude with an increase in the proportion of hydrogen in the fuel. Similar results were obtained in [8]. Despite this, at typical air temperatures at the inlet to the combustion chamber (600–800 K), the ignition delay time for lean hydrogen mixtures with air is about 100 ms, which is quite sufficient to organize the mixing process. Herzler, Lieuwen, and Beerer [13–15] showed that an increase in pressure also leads to a decrease in the ignition delay time of the methane–hydrogen mixture, as well as of pure methane (Figure 7).

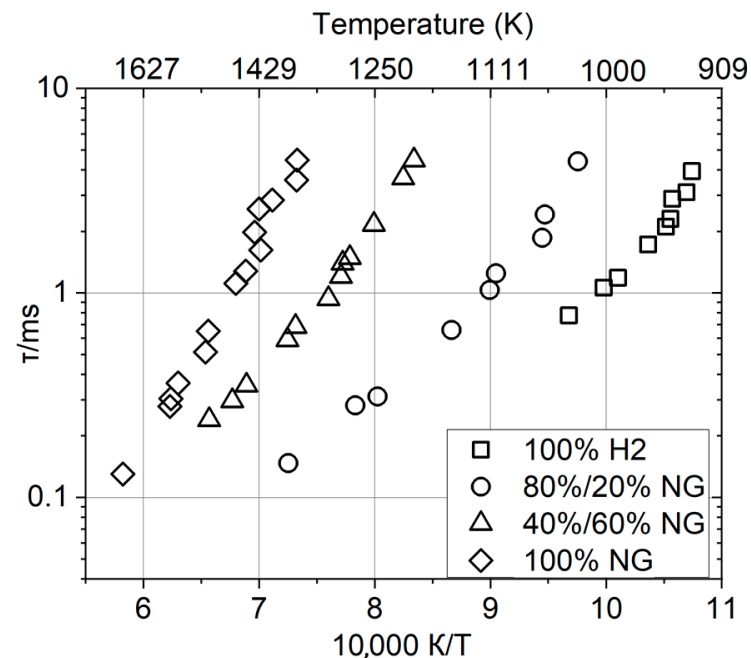


Figure 5. Change in the ignition delay time of a natural gas mixture depending on the volume fraction of hydrogen [13].

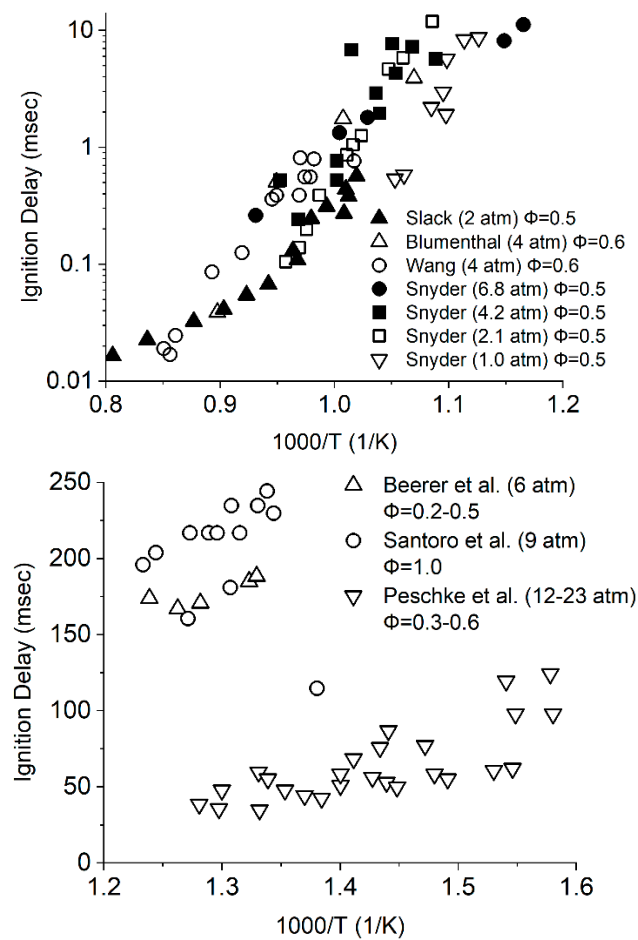


Figure 6. Change in the ignition delay time of a natural gas mixture depending on the volume fraction of hydrogen [14,15].

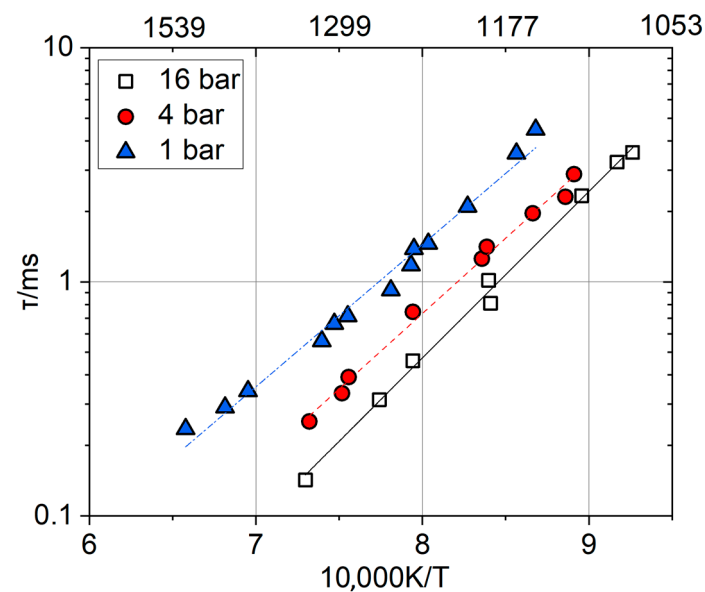


Figure 7. Change in the ignition delay time depending on pressure (experiment $\Phi = 0.5$, mixture of 40% H₂ and 60% natural gas by volume) [14].

According to our estimates (using a perfectly mixed reactor), the minimum temperature of hydrogen autoignition under atmospheric conditions with the residence time in the

reactor of 10 s is about 780–810 K (Figure 8), whereas according to Sun Y. et al. [10,16] (the autoignition induction time is 5 min) it is about 700 K, and for the stoichiometric mixtures of methane, it is about 850 K. The minimum autoignition temperature shifts to the region of rich mixtures and is approximately 70–150 degrees lower than that of methane [17,18]. It should be noted that the lower autoignition temperature of hydrogen leads to limitations in the use of lean premix combustion technology for power plants with a high temperature after compressors. Thus, for engines with the air temperature T_k of the order of 700 K and above, it is essential to use another combustion system, for example, a diffusion burner or a microcluster. At the same time, for engines with T_k below 700 K, the lean burn technology can still be used with high efficiency.

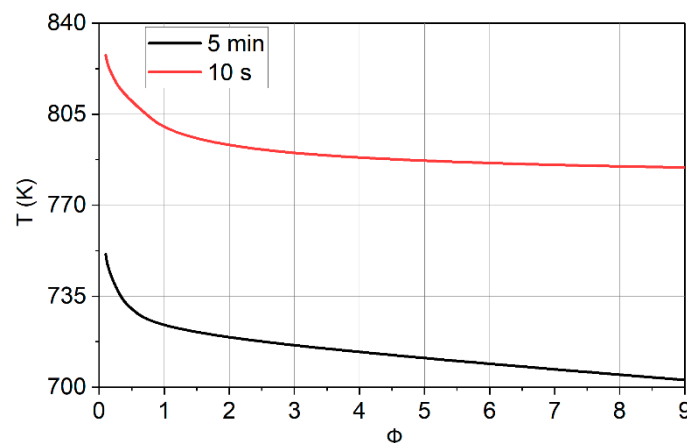


Figure 8. The influence of the equivalence ratio on the autoignition temperature.

Experimental studies in shock tubes have revealed a certain relationship between the high-temperature ignition and the pressure or fuel composition [19]. In the studies by Zhang and Gupta [17,18,20], three characteristic systems (modes) of ignition were identified, depending on the composition of the fuel:

- (1) MCDI (methane chemistry dominating ignition) system—for methane–hydrogen fuel mixtures containing less than 40% hydrogen, a decrease in the ignition delay time typical of hydrocarbons with increasing pressure is observed.
- (2) CCMHDI (combined chemistry of methane and hydrogen dominating ignition) system—for a 40% CH_4 /60% H_2 fuel mixture, there is no noticeable effect of pressure on the ignition time. In this case, the nature of ignition is determined neither by the kinetics of hydrogen nor by the kinetics of methane.
- (3) HCDI (hydrogen chemistry dominating ignition) system—the ignition typical of hydrogen and a complex pressure dependence that occurs when the mole hydrogen fraction of the mixture exceeds 80%.

2.4. Flame Size and Shape

The flame shape is an important characteristic that has an effect on the temperature field and pollutant emissions [21]. With a strong flow swirl, a typical flow structure is shown in Figure 9. The stream has two recirculation zones: the inner recirculation zone (IRZ) and the outer recirculation zone (ORZ). The fresh air–fuel mixture and combustion products are separated by an inner shear layer (ISL) and an outer shear layer (OSL). The flame is usually V-shaped if the combustion reaction occurs only at the boundary of the internal shear layer (ISL) of the fresh air–fuel mixture and the combustion products in the inner recirculation zone (IRZ). If the combustion process occurs at the boundary of the outer shear layer (OSL) of the fresh air–fuel mixture and the combustion products in the outer recirculation zone (ORZ), then the flame stabilizes with the M-shape. Thus, in the work by Choi [22], it was demonstrated that the M-shape flame is more prone to unstable

combustion than the V-shape. Changing the flame shape from M to V can increase its tolerance to pulsations.

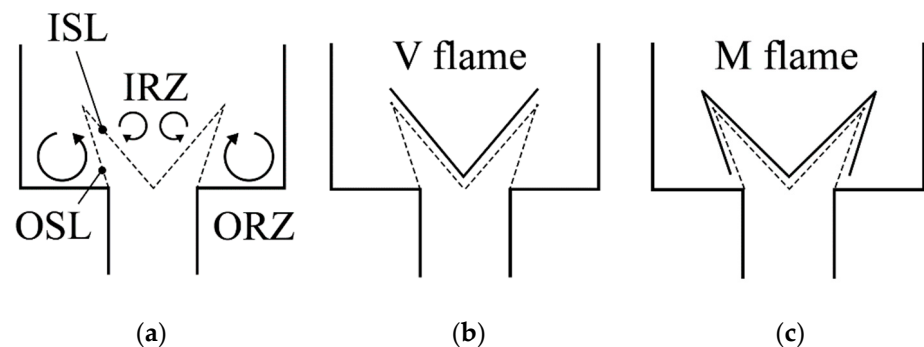


Figure 9. Scheme of swirling flow in the combustion chamber [21]: (a) graphical description of the inner and outer recirculation zones and internal shear layer; (b) V-shape flame; (c) M-shape flame.

The experimental study by Chterevev [23] is devoted to the effect of hydrogen enrichment of natural gas on the flame dynamics under atmospheric pressure conditions using a DLE (dry low emission) radially stepped burner. The volume contents of hydrogen were 0%, 5%, 11%, 21%, and 26%. The authors demonstrated that the flame shape changed along with the increased hydrogen percentage from M to V (Figure 10). Similar results were obtained in the paper by Figura [24], where a change in the nature of flame stabilization from an aerodynamically stabilized M-type to stabilization in a V-type shear layer was obtained when the fuel was enriched with hydrogen, and in the works by Yilmaz and Hu [25,26], where it was shown that the flame became more compact.

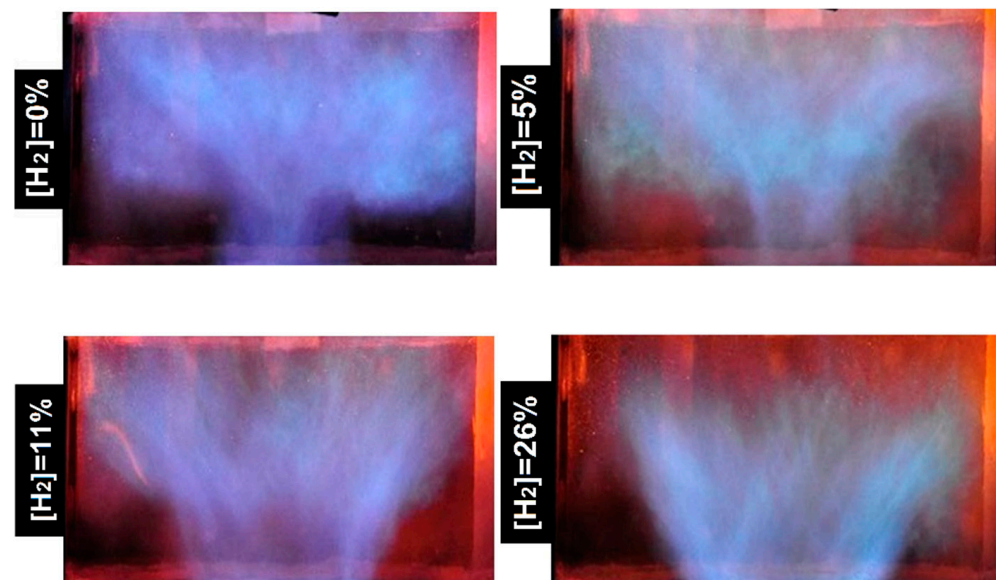


Figure 10. A change in the shape of the flame with the addition of hydrogen by volume [23].

Similar results were obtained in the paper by Indlekofer [27], where it was shown that the flame with a higher hydrogen percentage was characterized by a more compact shape, which indicates a better reactivity of the fuel mixture (Figure 11).

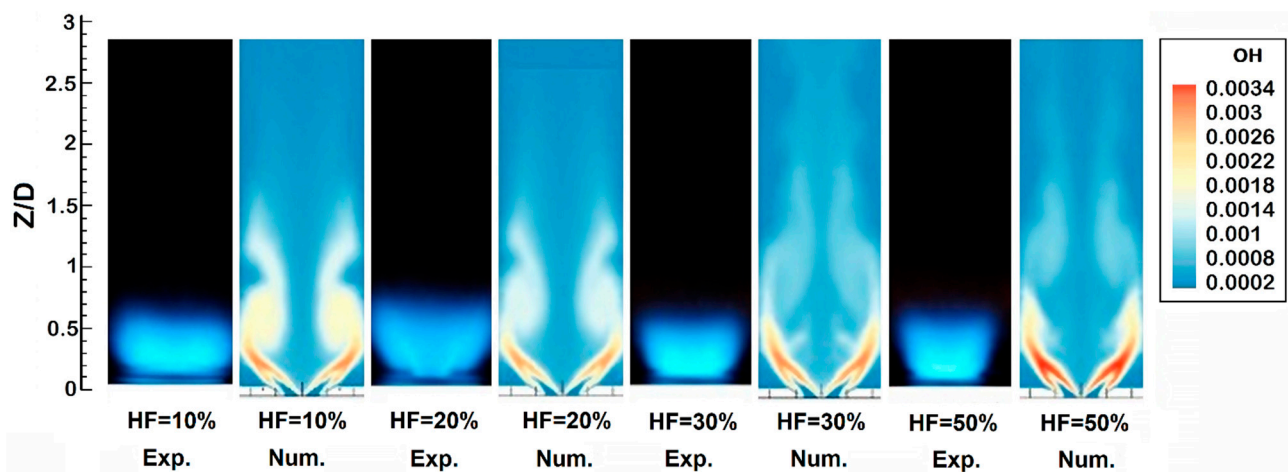


Figure 11. The flame shape in a swirled flow with various hydrogen additions by volume.

In the work of Wicksall [28], a premix fuel–air mixture was fed into a cylindrical chamber to explore the volume concentration range from 0 to 0.5 (where 0 is the absence of hydrogen in the mixture and 1 is pure hydrogen), which corresponds to the power fraction P_H from 0 to 0.25. The flame shapes for the two stable operating conditions are presented in Figure 12, which shows that with an increase in hydrogen content, the flame became more compact. At $P_H = 0.2$, the maximum heat release rate remained at the end of the flame brush. It also reduced the interaction with the neighboring flame, as evidenced by a much larger interaction area at $P_H = 0.1$. For the case of $P_H = 0.1$, it can be seen that the edges of the flames merged, which created a large vertically oriented area with a high heat release rate. This was not observed at $P_H = 0.2$, although there was some evidence of the flame tip interaction.

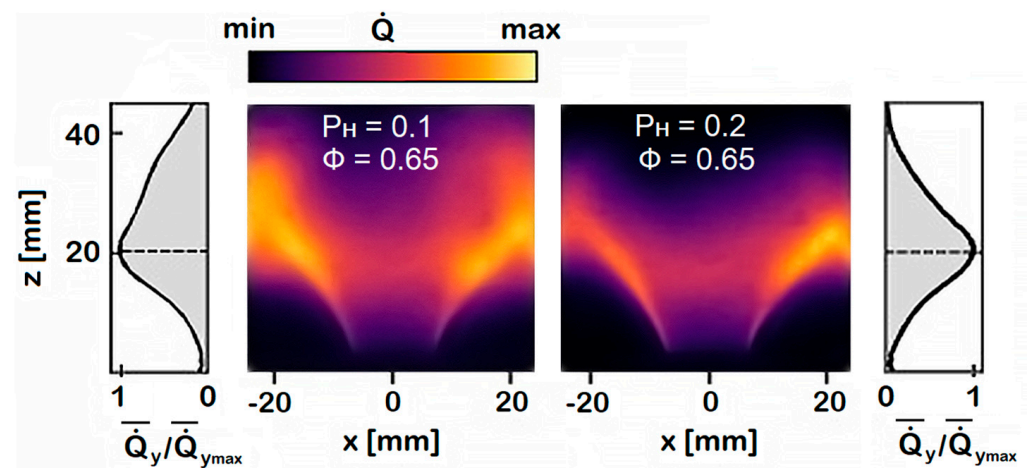


Figure 12. The average flame shapes and corresponding longitudinal distributions of the integral heat release rate for two stable operating conditions [28].

The study by Kashir [29] revealed that adding hydrogen at the volume content below 20% had little or no effect on the flame length, while when using the fuel with a hydrogen content of 40% by volume, the flame became much shorter (Figure 13).

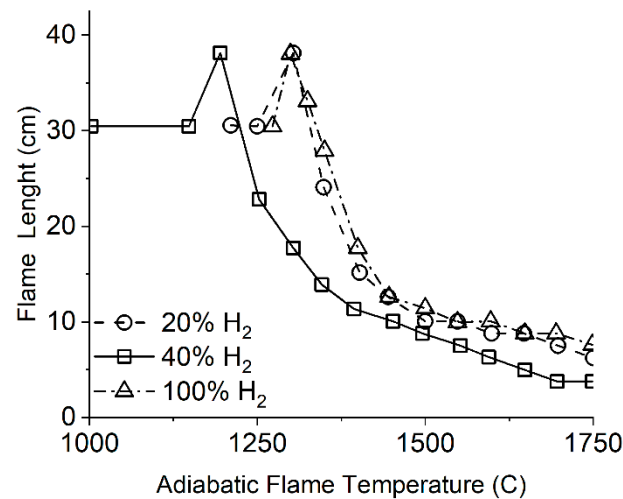


Figure 13. The relationship between the flame length and the temperature of adiabatic combustion at different volume contents of hydrogen [30].

The change in the shape of the flame is associated primarily with an increase in local heat release. As shown in the work by Bongartz [31], the flame became thinner with an increase in the hydrogen concentration in the methane–hydrogen mixture (Figure 14). This led to a change in the Karlovitz and Damköhler numbers, as was shown, for example, in the study by Zhang [32] (Figure 15). Thus, when hydrogen is added to the fuel, the combustion mode of a turbulent flame can be changed from the volumetric mode (when the smallest Kolmagorov turbulent scales penetrate into the flame) to the surface mode (when the turbulent vortices only distort the flame by changing its area but not the internal structure). This fact is one of the reasons for the change in the mechanism of the generation of pulsations during hydrogen combustion in comparison with methane combustion, which is considered below.

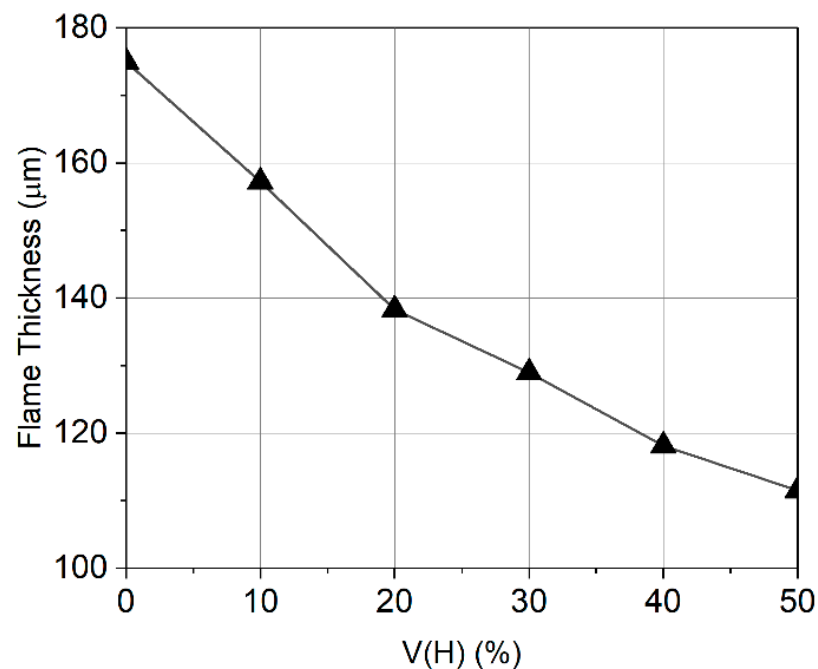


Figure 14. Flame thickness, depending on the volume fraction of hydrogen in the mixture [31].

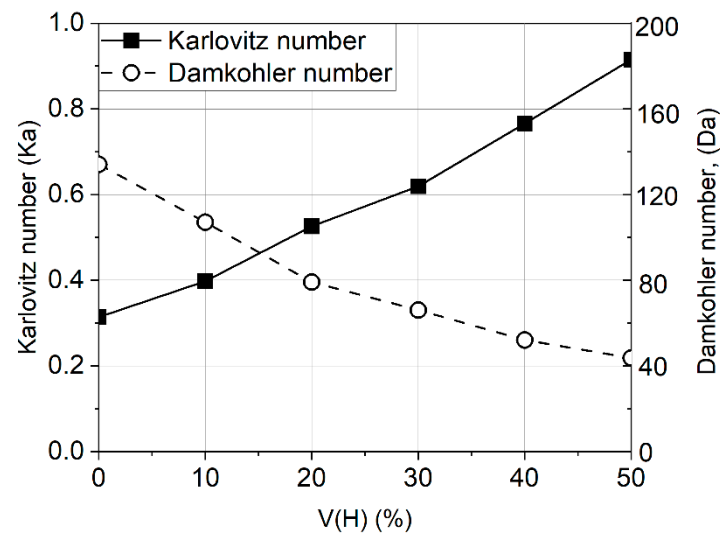


Figure 15. Karlovitz and Damköhler numbers for hydrogen volume fraction [31].

It is important to note that the change in these values (Ka and Da) has an effect on the results of calculations of the existing mechanisms [33,34]. Therefore, to predict the operation of hydrogen-fuel engines, some new or modified turbulent combustion models should be applied, as was suggested, for example, in the study by Bouras [35].

2.5. Flow Swirl

The size and intensity of the swirl in the central recirculation zone decrease as the axial velocity increases when hydrogen is added to the swirling flow of the preliminarily prepared mixture (hydrogen additions are up to 9% by weight) [36]. A higher reactivity of hydrogen reduces the amount of combustion products in the reverse currents [37], which reduces the supply of a colder working fluid and increases the temperature in the reaction zone.

Increasing the flow swirl reduces the temperature near the inlet to the combustion chamber, which is associated with an increase in the recirculation flow rate [38]. Kim [38] also noted that with an increase in the swirl number and the percentage of hydrogen in the fuel, the temperature in the reverse current zone decreased with a poor flameout, which led to a decrease in the energy for igniting the fresh mixture. Thus, with the addition of hydrogen, an increase in the swirl of the flow led to an increase in the adiabatic temperature of the flame at lean blowout.

The stronger the swirling of the flow, the smaller the effect of hydrogen additions on the formation of NO due to an increase in the proportion of combustion products in the combustion zone [38].

3. Influence of the Behavior Features of the Hydrogen Combustion Processes on the Characteristics of Combustion Chambers

3.1. Formation of Pollutant Emissions: CO and CO₂

One of the main benefits of using hydrogen is to reduce the carbon footprint of power plants. A decrease in carbon concentration in the initial fuel leads to an unambiguous decrease in CO₂ in the combustion products per unit of the heat received (or per unit mass of the fuel). For example, Leng [39] reports a considerable CO and HC emission reduction that is achieved already at the H₂ 10% content, which is related to an increased combustion efficiency. With the further H₂ increase, the CO and HC reduction is not so considerable, which is related to a decreased CO content in the fuel. However, when burning the methane–hydrogen mixtures, changes in CO concentration in the combustion products do not behave so unambiguously. Thus, Bouras [35] and Abubakar [40] report on the increased CO concentration in the combustion products (Figures 16 and 17).

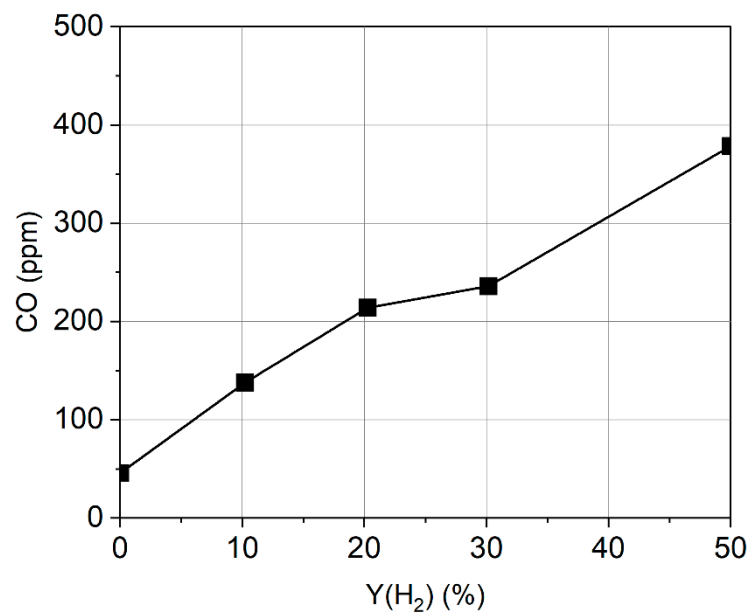


Figure 16. Dependence of CO emissions on the molar concentration of hydrogen in methane–hydrogen mixture [35,40].

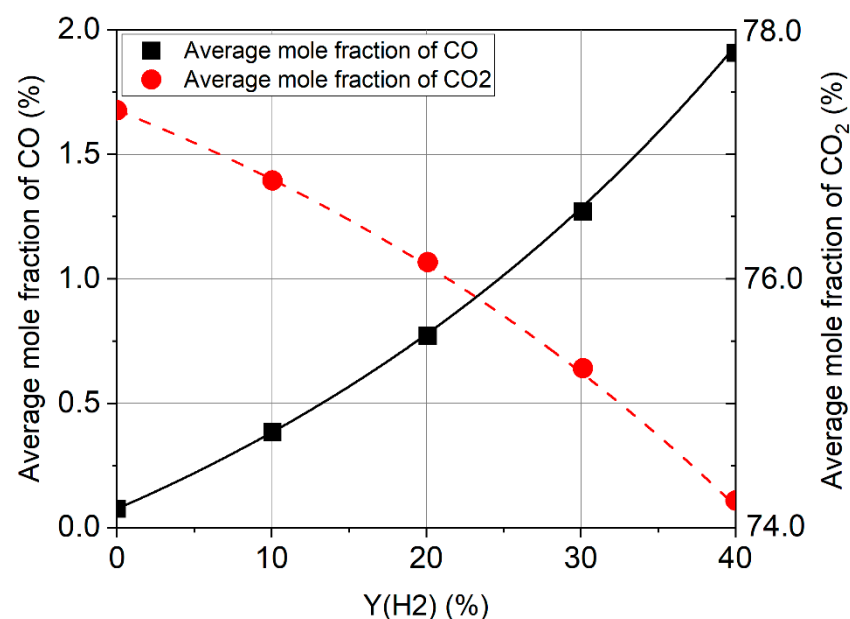


Figure 17. Dependence of CO and CO₂ emissions on the molar concentration of hydrogen in a hydrogen–butane mixture [41].

An increase in CO emissions with an increased hydrogen concentration may be partly due to a shorter residence time of gases in the combustion chamber at higher hydrogen concentrations. Another reason for an increase in CO emissions with hydrogen enrichment is that, due to a higher reactivity and adiabatic flame temperature of hydrogen compared to hydrocarbon fuels, the hydrogen enriched fuel mixtures will burn more efficiently. Therkelsen [41] also reports that high temperatures (above the CO₂ dissociation threshold), during the combustion of hydrocarbons, stimulate CO conversion and therefore lead to a more complete combustion and lower CO emissions. However, despite all this, competition for oxygen between highly reactive hydrogen and hydrocarbons in the mixture can contribute to an increased CO emissions [42]. In other words, hydrogen inhibits the oxidation of hydrocarbons and their intermediates in an environment with a limited oxygen

content (stoichiometric or rich). The competition described above disappears when burning lean mixtures, as shown in Figure 18.

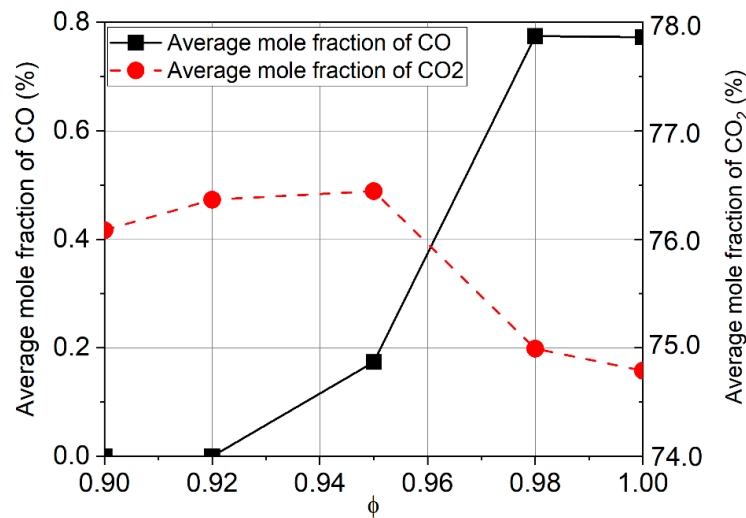


Figure 18. CO and CO₂ emissions for various equivalence factors [41].

3.2. Formation of Pollutant Emissions: NO_x

NO_x emissions consist mainly of nitric oxide (NO) and, to a lesser extent, of nitrogen dioxide (NO₂) and nitrous oxide (N₂O). Being a precursor to photochemical smog, NO_x also contributes to acid rain and causes ozone depletion, which makes it a pollutant regulated by national and international organizations, specifically by ICAO.

In a laminar flame and at the molecular level in the turbulent flame, the formation of NO_x can be explained by four different chemical kinetic processes: thermal NO_x, fast (instantaneous) NO_x, fuel NO_x, and N₂O intermediate. Thermal nitrogen oxides are formed as a result of oxidation of the nitrogen present in the atmospheric air supplied for combustion; instantaneous nitrogen oxides are formed during high-speed reactions in the flame front, and fuel nitrogen oxides are formed in the process of oxidation of the nitrogen contained in the fuel. Under high pressure and oxygen-rich conditions, NO_x can also originate from molecular nitrogen (N₂) via N₂O.

Hashemi [42] and Ghoniem [43] present the results of the studies into various mixtures of natural gas and hydrogen that show an exponential increase in NO emissions as the percentage of hydrogen increases (Figure 19). Chen and Kim [44,45] also report on the increased NO_x emissions when adding hydrogen.

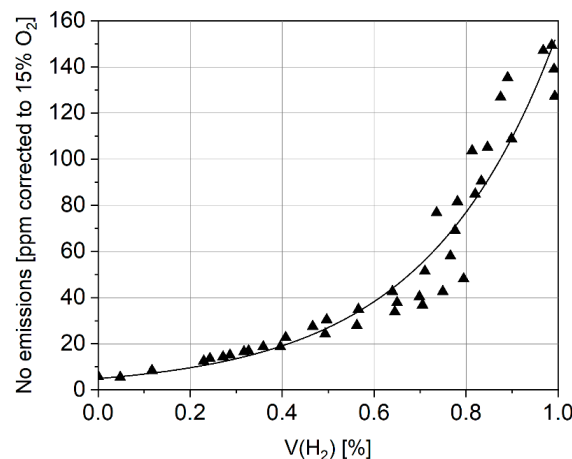


Figure 19. The relationship between the NO emissions of natural gas and hydrogen and the volume fraction of hydrogen.

Figure 19 shows that there is a significant increase in the rate of NO formation between 60% and 100% hydrogen, which in this study was most likely due to an increased rate of hydrogen formation by means of the thermal mechanism. However, in the studies by Griebel [4] and Semenikhin [46], the data were normalized to the same temperature in the flame front, which proves the fact that at the same combustion temperature, the concentration of nitrogen oxides in the combustion products of methane–hydrogen mixtures is higher than when burning pure methane (Figure 20). This may be due to both a decrease (compactification) of the flame front (which leads to an increased gas residence time in the high-temperature region) and to a change in the chemical mechanism of the nitrogen oxide formation. Thus, the problem of validating the kinetic mechanisms of the nitrogen oxide formation during hydrogen combustion becomes critical, as is described, for example, in the paper by Papanikolaou [47].

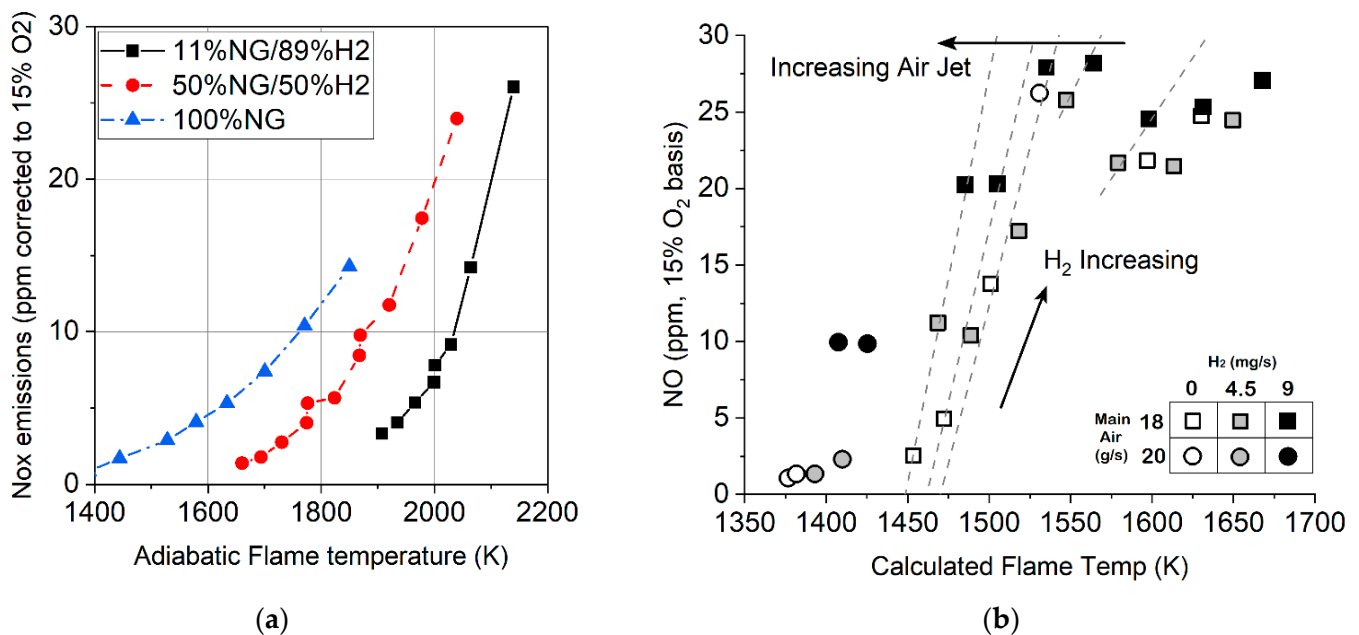


Figure 20. Dependence of NOx emissions on the adiabatic flame temperature for different volume proportions of hydrogen–natural gas [4,47] (a) for methane–hydrogen mixtures with constant methane consumption; (b) for methane–hydrogen mixtures with different methane consumptions.

3.3. Flame Blowout and Flashback

The reliability of the combustion chamber is determined by characteristics such as lean flame blowout, flashback, and pulsating combustion. Adding hydrogen to methane significantly increases the blowout limits of both the suspended and the attached diffusion flames [48,49] (Figure 21). The effect of adding hydrogen to the air flow is much more pronounced than that of adding it to methane (with a separate fuel supply). Figure 21 shows that the flow velocity stabilization limits are proportional to the square of the maximum laminar flame propagation velocity. Adding the diluents (CO₂ and N₂) to the fuel reduces the resistance of the diffusion flame to a much greater extent for the suspended flame than for the attached flame.

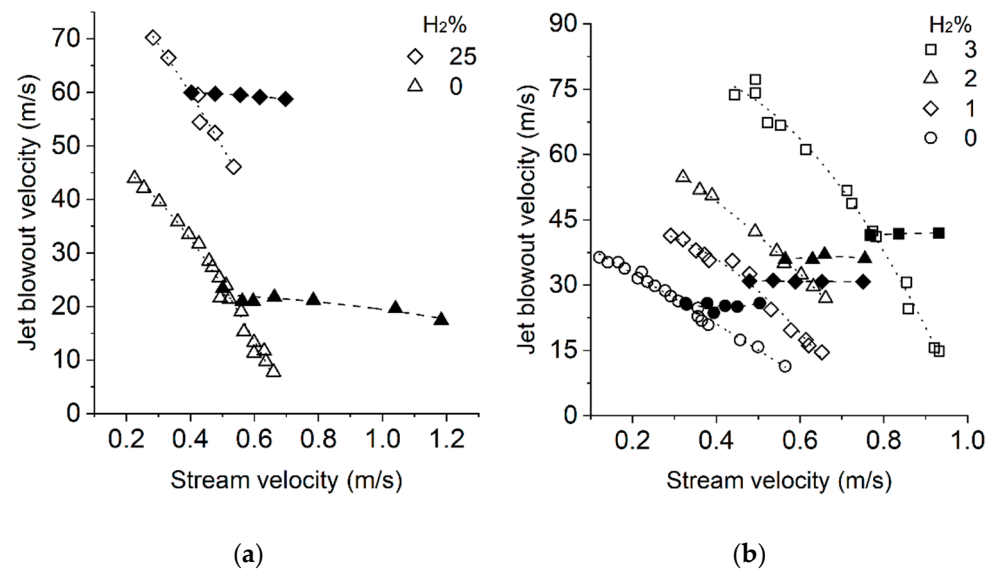


Figure 21. Flame blowout during combustion of methane and hydrogen–methane with different volume fractions of hydrogen [48,49]: (a) for methane–hydrogen fuel jet and air stream; (b) for methane fuel jet and air–hydrogen stream.

Zhu [50] (Figure 22) presents a study into stabilization of the flame of a premixed methane–air mixture with hydrogen additives (up to 29% by mole fraction) behind a bladed swirler. It was shown that an increased combustion stability upon hydrogen enrichment was a direct result of higher concentrations of OH, H, and O radicals, which led to an increase in several key reaction rates. In this case, the flame extinction time was influenced not only by the value of the average OH concentration but also by its RMS [51]. The greatest effect was achieved with small additions of hydrogen (up to 12–20% [52] by mole fractions), while an increase to 29% by mole fractions was not so pronounced, although it had a further positive effect on the combustion stability.

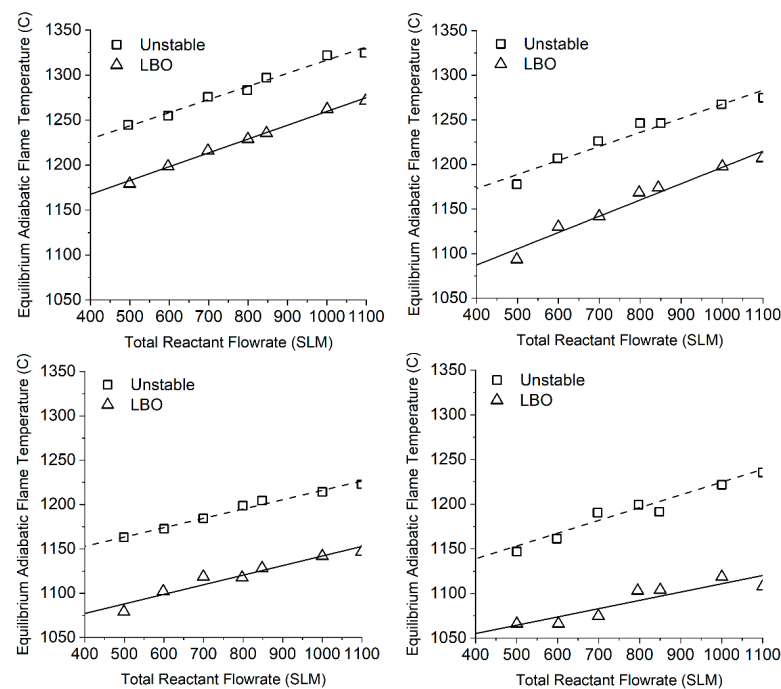


Figure 22. Change of adiabatic flame temperature during flame blowout.

Schefer [51] (Figure 23) reported that the addition of hydrogen to methane up to 20% by volume reduced the equivalence ratio during the blowout of a homogeneous flame by 9–10%, and the relationship between the Φ blowout and the volume content of hydrogen in the fuel was linear, which was also confirmed in Schefer [49]. However, in [49], the effect of H_2 on the flame blowout was more significant and amounted to about 15–20% Φ for every 20% addition of hydrogen.

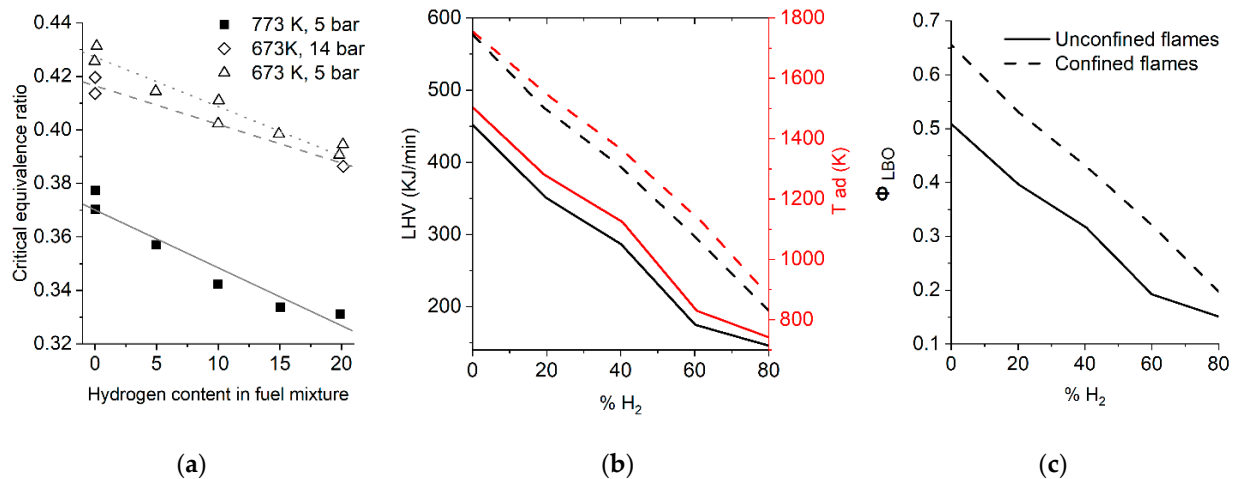


Figure 23. Influence of hydrogen volume fraction on lean flame blowout: (a) [52]; (b) [50]; (c) [50].

Griebel and Choi [52,53] present a map of the combustion regimes of a methane–hydrogen premix mixture with air. It was found that with an increase in the percentage of hydrogen, the limits for flame blowout and flashback were shifted to a leaner region, which was associated with an increase in the flame speed and a decrease in the ignition delay time. In this case, the flame can burn at lower temperatures, as shown in Figure 24. Confirmation of this can also be found in the study by Wicksall [28], where at the 40% hydrogen content, the temperature of the lean flame blowout was significantly reduced.

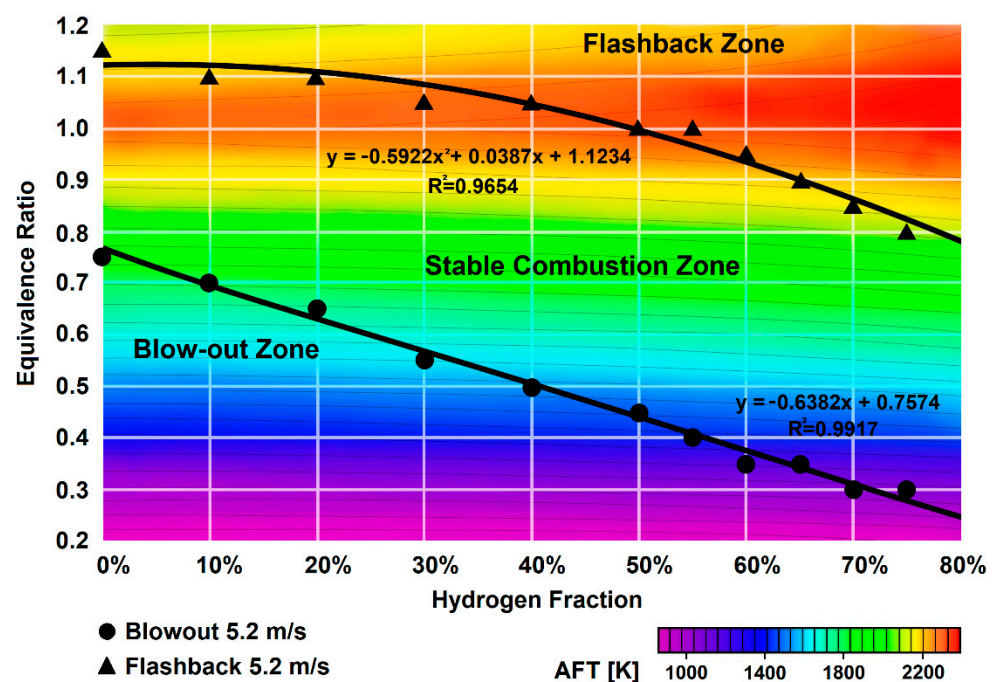


Figure 24. The influence of the volume concentration of hydrogen on the boundary of sustainable combustion for the lean flame blowout and flashback [28].

Wicksall [28] also showed that the flame blowout to some extent correlated with the Reynolds number, which was determined by the influence of the flow turbulence intensity. In this case, an increase in the hydrogen percentage in the mixture led to a decrease in the Reynolds number while maintaining the constant flow rate.

Nemitallah [34] reports that with an increase in the percentage of hydrogen in the fuel, the role of the external (corner) recirculation zones in flame stabilization decreased, since the flame was shifted closer to the place of fuel supply. With the addition of hydrogen, the lean flame blowout limit decreased linearly, resulting in stable flame at lower flame temperatures.

When methane was enriched with hydrogen at the ratio of 55%, the flame had the widest stable range (Figure 25). Any attempt to increase the hydrogen percentage above 55% under stoichiometric conditions (the equivalence factor 1.0) failed, and the flame went out due to flashback. This is different to the flame of pure methane, which has been proven to be stable under stoichiometric conditions. Increasing the hydrogen percentage in the fuel mixture increases the laminar flame speed, and the flame is propagated upstream from the reactant gases, resulting in earlier ignition compared to the oxygen flame of pure methane.

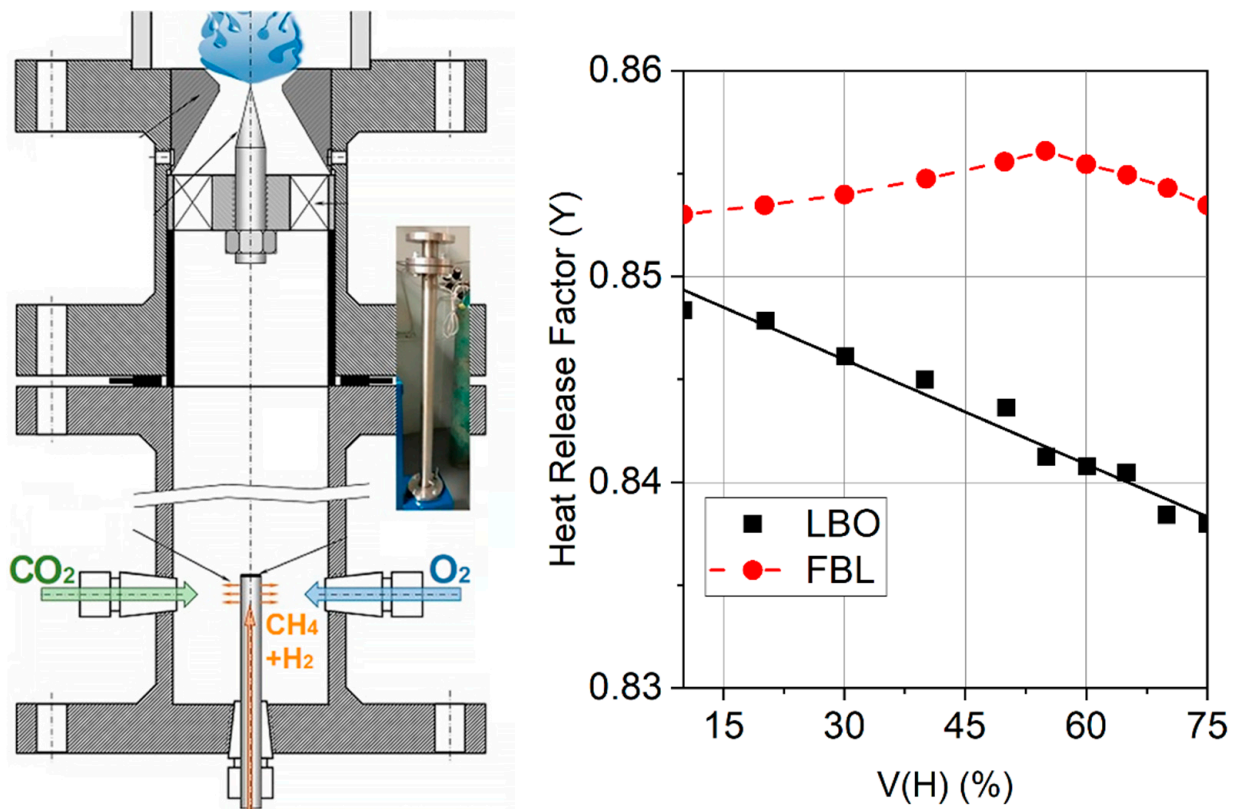


Figure 25. The range of burner stable operations with the hydrogen added to the fuel by volume.

One of the main factors determining the expansion of the combustion limits for lean flame blowout with the addition of hydrogen is an increase in the critical flame deformation rate. Nemitallah [34] has shown that the critical strain rate significantly increased by over two times from $\approx 4300 \text{ s}^{-1}$ for the combustion of pure methane to $\approx 9700 \text{ s}^{-1}$ to expand the boundaries of stable combustion (Figure 26).

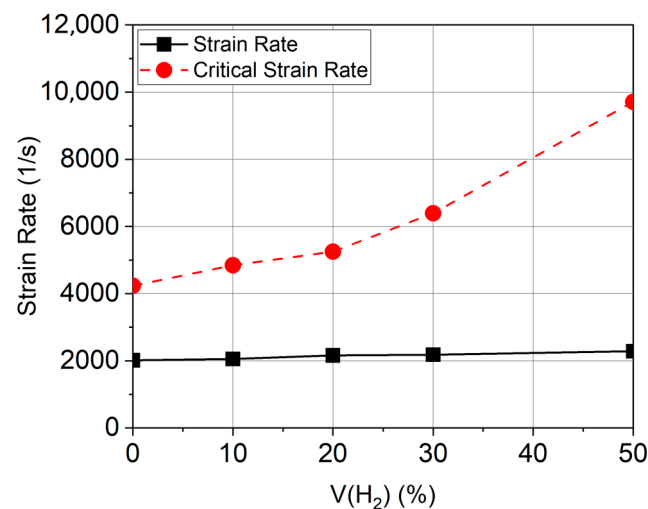


Figure 26. Change in the critical strain rate in the flame and the strain rate in the flow with a change in the hydrogen volume fraction in the fuel [34].

Thus, almost all studies confirm the positive effect of hydrogen additions on the resistance of the lean flame blowout. Moreover, it increases the probability of flashback. In general, the range of stable operation shifts to the region of lean mixtures, and the operating window expands in terms of the excess air coefficient, reaching its maximum value at $HF \approx 0.55$. It is important to note that when hydrogen is added, the working window shifts towards lower flame temperatures, which contributes to a decreased rate of nitrogen oxide formation. Therefore, one of the main recommendations when converting combustion chambers to hydrogen is the need to ensure that the temperature in the combustion zone is 100–200 degrees lower (depending on the hydrogen concentration) than when burning methane.

3.4. Unsteady Combustion

Pulsations in the combustion chamber are often undesirable since they can cause its complete destruction. At present, the mechanisms of pulsation generation during natural gas combustion are well described. It has been established that there are no fundamental changes in these mechanisms during hydrogen combustion; however, since the flame characteristics change, they can transform the mechanisms for generating pulsating combustion. The purpose of this section is to analyze the works devoted to the effect of hydrogen additives on unsteady combustion. In this case, several areas of analysis of the effects of hydrogen addition can be distinguished: time-lag, the shape and position of the flame, changes in frequency and amplitude, and changes in the phase delay.

With an increase in the hydrogen content, the shape, size and location of the flame change significantly. As shown in [21,23,25,27,34,54–59], the flame becomes more compact (shorter) and pressed against the base of the burner. During combustion of a premix mixture in the swirling flow, the shape of the flame changes from M to V. According to Wicksall [28], this change in size can occur when the percentage volume of hydrogen is over 20%. Chterevev [23] and Kashir [29] demonstrate that a decrease in the size of flames in an annular combustion chamber leads to a decrease in the probability of their interaction with each other and, consequently, to the elimination of the mechanism for pulsation generation. This impact on the size and location of the flame is explained by an increase in the local heat release and the temperature in the combustion zone along with an increase in the hydrogen content in the fuel–air mixture. It is also worth noting that the addition of hydrogen leads to a change in the flame stabilization region [25], modifying the nature of the flame from the suspended to a more stable flame with a fixed stabilization point. In that instance, the most stable option would be a fixed point of stabilization of the flame through the use of a pilot circuit or a bluff body with a fixed separation point.

Davis [55] has shown that the transition to harmonic oscillations is preceded by the appearance of a flame in the outer recirculation zone, which, for the combustion of methane–hydrogen mixtures, occurs at leaner fuel–air mixture compositions than during methane combustion. This transition can be estimated using the function of the dimensionless strain rate (normalized strain rate): $\frac{k_{ext}D}{U_{\infty}}$. In the article by Figura [24], a “center of heat release” was proposed as an indicator of stability, because a flame having the same “heat center” location but different operating conditions and fuel composition has almost the same shape.

Chterelev [23] studies the effect of adding hydrogen to a lean mixture of natural gas with air during combustion of a premixed mixture in a swirling flow. The hydrogen percentage in the fuel–air mixture varied up to 50% by volume. As a result, the influence of hydrogen addition on the shape of the flame, the characteristics of the structure of the precessing vortex core (PVC), and the frequency and amplitude of pulsations had to be investigated. Regarding the thermoacoustic characteristics, it was found that with an increase in the percentage of hydrogen in the fuel (as well as an increased air temperature), the speed of sound between the fuel supply point and the flame front (in the premixer) increased due to a decrease in the average molecular weight of the mixture with the addition of hydrogen (Figure 27). This characteristic reflects the transfer time of the acoustic energy from the flame front, as a source, to the place of fuel supply, as a factor that further leads to an increase in pulsations. Thus, both the addition of hydrogen and a decrease in the flame size lead to a decrease in the time of acoustic energy transfer from the flame front to the place of fuel supply, transforming and increasing the pulsation frequency [23]. In this event, the pulsation frequency with an M-type flame is lower than that with a V-type.

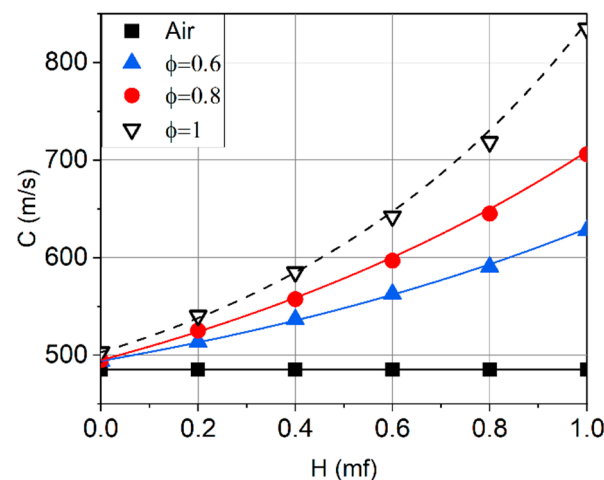


Figure 27. The influence of the molar fraction of hydrogen on the speed of sound.

Similar conclusions were obtained in the study by Imteyaz [60] devoted to the effect of adding hydrogen to the methane–air mixture on the self-excited thermoacoustic instability of the flame, including the case when the length of the combustion chamber was changed in the range from 300 to 1100 mm. With an increased percentage of hydrogen, the size of the flame also decreased (Figure 28). At a low hydrogen concentration ($\approx 15\%$), excitation took place mainly for low-frequency primary acoustic modes (< 200 Hz). When the frequency of the primary oscillations (without addition of hydrogen) was below 200 Hz, the frequency tended to increase linearly with the percentage of hydrogen. However, the linear relationship between the frequency and the hydrogen fraction was associated with acoustic modes that are influenced by the chamber length. At high hydrogen concentrations ($> 40\%$), the primary acoustic modes tended to occur at higher frequencies (≈ 400 Hz). Furthermore, increasing the hydrogen content leads to a decrease in flame length (Figure 28).

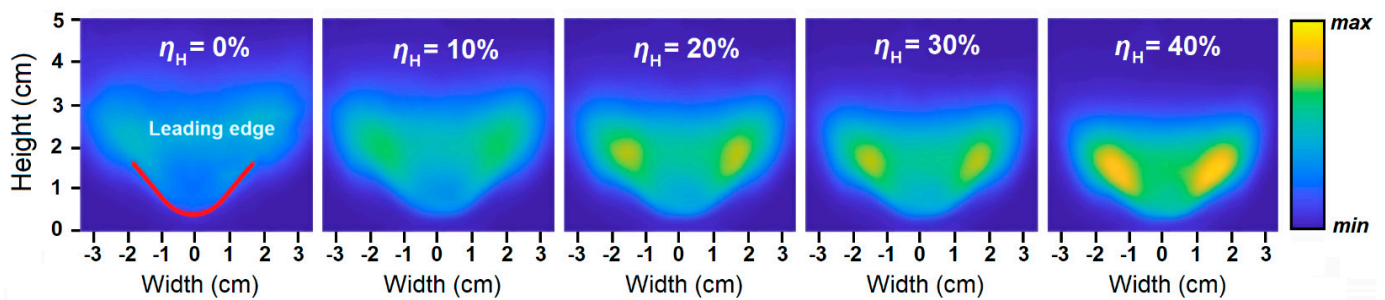


Figure 28. The relationship between the flame length and the hydrogen volume fraction [60].

In the papers by Zhang and Davis [54,55], the observed frequencies coincided with the frequencies of the longitudinal modes of the chamber, while in [54], the hydrogen content had no effect on the pulsation frequency, which remained equal to the frequency of the first longitudinal mode of the combustion chamber. On the other hand, in [23,60], the authors noted an increase in the frequencies of the first modes with an increase in the hydrogen content due to an increase in the temperature of the combustion products and, as a consequence, an increased sound speed in the combustion chamber. While maintaining the temperature of the combustion products, the pulsation frequency can remain the same.

Wicksall [28] reports that with an increase in the fraction of the hydrogen content, the acoustic energy is redistributed between frequencies. Thus, when burning pure methane, the authors identified the three main frequencies of 275 Hz, 450 Hz, 600 Hz, while for burning 60% of hydrogen, the only frequency characteristic was 450 Hz. The absence of the 600 Hz band indicates a change in the acoustic damping/amplification characteristics (amplitudes) of the combustion chamber, providing a high intensity in the 450 Hz band. This combustion mode is more dangerous since it can lead to the fatigue failure of the elements of the combustion chamber.

Davis [55] reveals that, upon transition to the oscillation mode, the pulsation frequency during the combustion of a hydrogen–methane mixture was equal to the pulsation frequency during the combustion of pure methane (110 Hz). However, at an excess air ratio of 0.65, the instability in the combustion of the hydrogen–methane mixture escalated to a higher frequency of 180 Hz. All the observed frequencies (110, 180 Hz) coincided with the frequencies of the longitudinal modes of the combustion chamber.

The relationship between the hydrogen content and the amplitude of pressure fluctuations depends on the design and operating parameters of the combustion chamber: its length, the average pressure, excess air coefficient, acoustic conditions at the inlet and outlet of the chamber, the swirl number, etc.

Imteyaz [60] states that a low hydrogen content ($\approx 15\%$) can enhance pulsations, while a sufficiently high hydrogen level ($\approx 40\%$) can weaken the primary modes. In turn, in the study by Indlekofer [27], the largest amplitude was found at 25% hydrogen content in the fuel by volume and decreased with a further increase in the hydrogen content. When studying the combustion of a premixed mixture in a swirling flow, Wicksall [28] found that the noise level was practically independent of the volumetric content of hydrogen, with the exception of a fuel–air mixture with a hydrogen content of 40% at an adiabatic temperature $T_{ad} > 1500^\circ\text{C}$. These results indicate a transition from the stable combustion regime to the unstable one with an increase in the hydrogen volume concentration. Ge [21] observed a decrease in the amplitude of pulsations in the entire range of hydrogen content studied (5–26% by volume). The explanation of the multidirectional influence of hydrogen addition can be related to the initial phase delay between the heat release pulsations and the pressure pulsations (Figure 29). If, during the combustion of methane, the phase delay was negative, i.e., the pressure pulsations occurred after the heat release pulsations (at the phase angle of $0 > \varphi > 90$), adding hydrogen would increase the amplitude of pulsations. If in the initial configuration without hydrogen, the phase delay was positive, i.e., pressure pulsations occurred before heat release pulsations (at a phase angle of $0 > \varphi > 90$), adding

hydrogen would reduce the pulsation amplitude. If, in the initial configuration, the acoustic pressure and changes in heat release were in phase, any change in the hydrogen content could reduce the pulsation amplitude, which means that the pulsation frequency would generally increase.

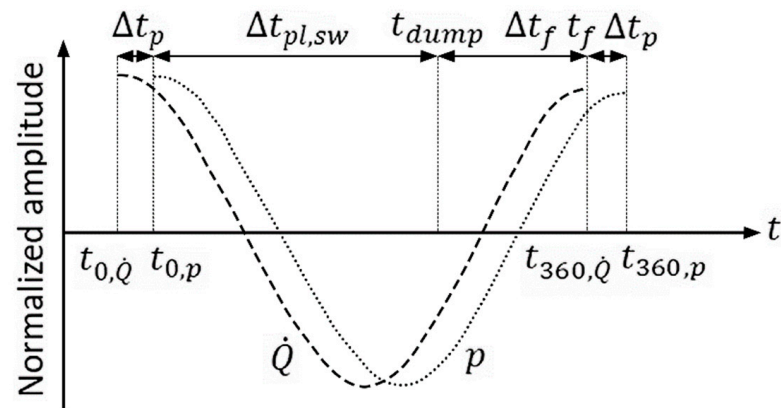


Figure 29. The scheme of the amplitude of pressure fluctuations in the fuel–air mixture flame.

With an increase in the hydrogen content, the frequency distribution of the power spectral density can change [28]. At the same time, significant changes in the pulsation amplitude occur when hydrogen is added to the fuel from 30–40% of volume and above.

This implies [24] that the dynamic stability of the combustion chamber with a change in the composition of the fuel and operating conditions is largely determined by the position of the center of the heat release flame (the middle location of the flame) under stable conditions.

3.5. Lewis Number

It is worth noting the decrease in the thickness of the flame with an increase in the concentration of hydrogen in methane–air mixtures (Figure 30). This leads to a change in the Karlovitz and Damköhler numbers (Figure 31), which entails changes in the regimes along the Borghi diagram, as shown, for example, by Zhang [61].

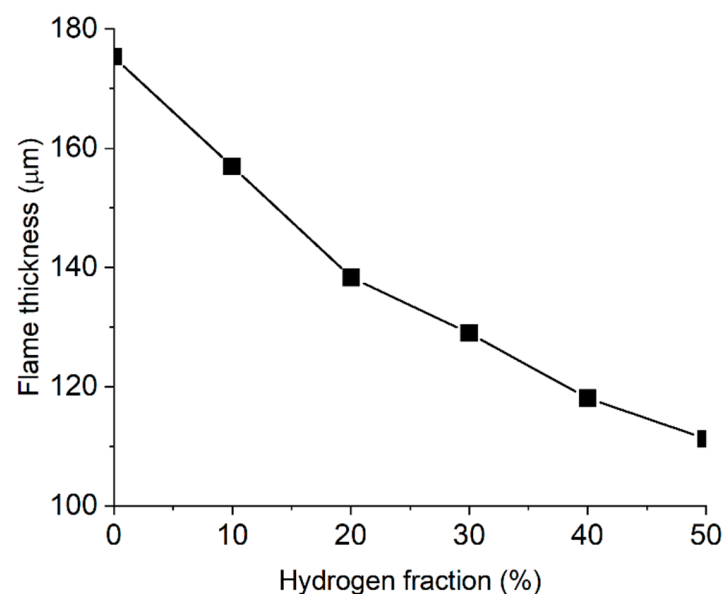


Figure 30. The curve of dependence of flame thickness on the volume fraction of hydrogen in the mixture [30].

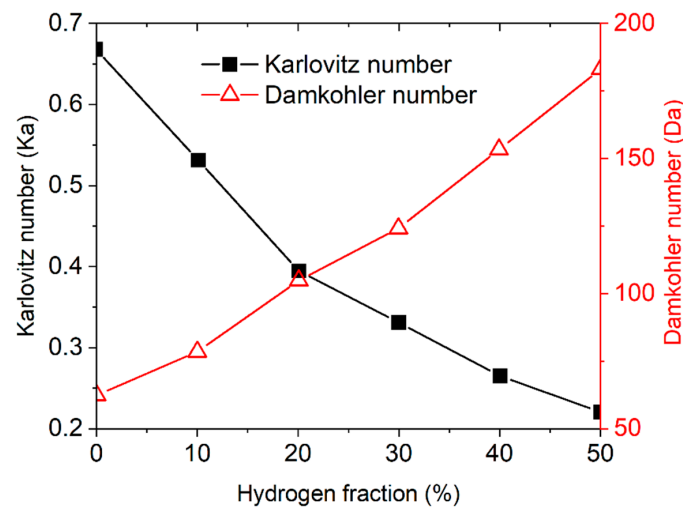


Figure 31. The curves of dependence of the Karlovitz and Damköhler numbers on the volume fraction of hydrogen in the mixture [30].

At $Ka < 1$, the thickness of the laminar flame is less than the smallest (Kolmagorov's) vortices. This means that small vortices can only distort the shape of the flame and not penetrate into the interior of the flame to change its structure. Thus, the hydrogen flame front is more prone to distortion than hydrocarbons [62].

It was shown in the work of Aspden [63] that the Lewis number had a greater effect on the combustion rate of hydrogen, in contrast to the combustion of methane, propane, and other hydrocarbons. The range of the Lewis number during the combustion of hydrogen is shown in Figure 32 [64]. Determination of a universal method for estimating the effective Lewis number for fuel mixtures requires further study and generalization, since the existing data lead to conflicting conclusions due to the difference in combustion modes [65].

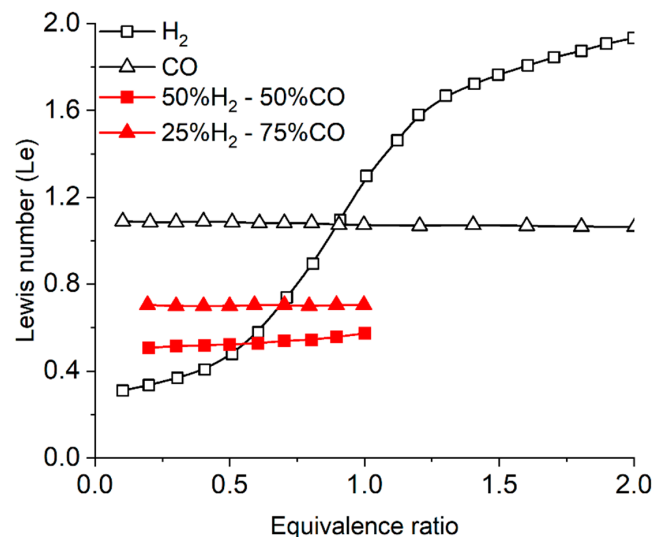


Figure 32. Curves of dependence of the Lewis number on the equivalence ratio (composition of mixtures in volume fractions).

In turn, in one of the widely used turbulent combustion models FGM, it is not possible to change the Lewis number for Flamelet generation, which remains one of the main limitations in applying this approach to modeling hydrogen combustion processes.

The local burning rate in a methane flame is relatively insensitive to flame curvature, while the data from the work by Bell [66] show a very strong positive correlation of flame speed with positive curvature and a weaker positive correlation with negative

flame curvature (Figure 33). For a thermodiffusion-unstable hydrogen flame, combustion intensifies in regions of positive curvature and has pockets of local extinction at negative curvature. Dinkelacker [65] revealed that the hydrogen flame velocity is determined by the front part (from the side of unburnt reagents) of the curved front, while the back part of the flame plays the role of the burnout zone. Later, Lipatnikov [67] developed this concept for the leading point model [67]. Thus, the effects of molecular diffusion play an important role in the combustion of fuels containing hydrogen.

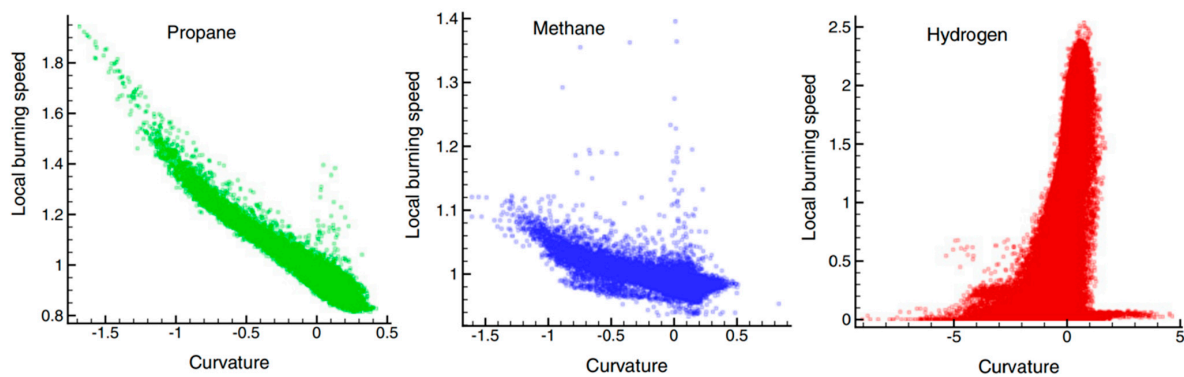


Figure 33. Correlation of local burning speed with curvature for each flame. Flame speeds are normalized to the corresponding laminar burning speed, and curvature is normalized with the laminar flame thermal thickness.

For a propane flame, the diffusion coefficient of the fuel is much less than the thermal conductivity, which allows the fuel to heat up faster than it diffuses into the flame zone. This causes the curve of the dependence of the molar fraction of fuel on temperature in Figure 34 to shift so that it is higher than the methane curve. The diffusion coefficient of hydrogen is higher, which leads to an increase in the diffusion of fuel into the flame and a downward shift in the dependence of the mole fraction of fuel on temperature. Aspden [68] demonstrates that as turbulent velocity fluctuations increase, turbulent diffusion begins to dominate molecular diffusion, and the curves of the dependence of the molar fraction of fuel on temperature become similar to the curve for methane (Figure 34), and thus we assume that the propane curve would do same. Since the burning rate increases as the fuel concentration and temperature increase as the flame becomes distributed, it can be expected that the burning rate decreases in the case of a high Lewis number and increases in the case of a low Lewis number.

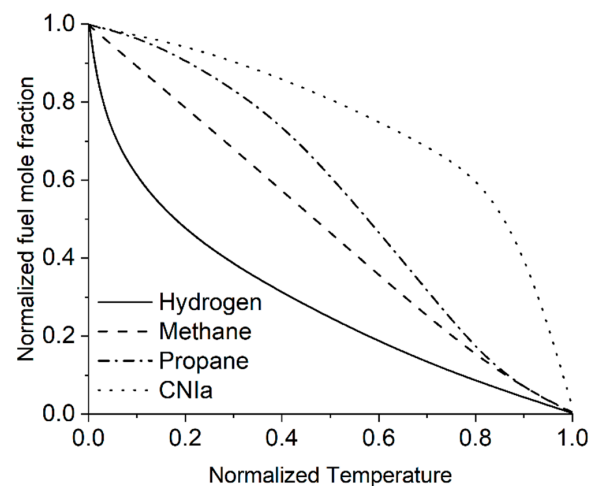


Figure 34. Distribution of normalized temperature and fuel mole fraction for four fuels with different Lewis numbers.

4. Conclusions

The analysis of the literature studying hydrogen combustion has resulted in the following conclusions and recommendations:

- The density of hydrogen is almost an order of magnitude lower than the density of natural gas, whereas the net calorific value per cubic meter is much lower. Thus, while maintaining the parameters of the power plant when switching to hydrogen, it is necessary to pay attention to the flow sections of the fuel supply system, especially to the fuel injectors.
- The addition of hydrogen leads to an increased intensity of chemical processes per unit volume in the flame front. This results in the compactification of the flame, a change in its shape, and a decrease in its size.
- The adiabatic combustion temperature of hydrogen flame is 5–15% higher than that of methane; however, the operating range of hydrogen covers some lower minimum temperatures of up to 1050 K, compared to ≈ 1400 –1500 K for methane, due to the high concentration of active radicals (H, HO).
- The addition of hydrogen results in a significant increase in the flame propagation speed. The greatest effect is achieved at a hydrogen concentration in the fuel of 65% or more. In this case, the maximum velocity shifts to the region of rich mixtures. On a basis of high hydrogen velocity, the combustion chamber can theoretically be shortened, which will reduce both the engine weight and NO_x emissions by cutting the residence time of the air–fuel mixture in the high-temperature zones.
- To ensure combustion with no flashbacks, it is necessary to increase the flow rate, which requires an increase in the pressure drop across the flame tube head and, in general, an increase in pressure losses in the combustion chamber.
- The ignition delay time of hydrogen is of several orders of magnitude shorter than that of methane. The minimum autoignition temperature shifts to the region of rich mixtures and is approximately 70–150 degrees lower than that of methane. Thus, for combustion chambers with the air temperature $T_k > 700$ K, it is advisable to use a combustion system without premixing, for example, LDI or a multicluster.
- The CO emission increases when hydrogen is added to the fuel, while CO₂ decreases for stoichiometric and rich mixtures. Burning lean mixtures of hydrogen with air allows a reduction in the level of CO and CO₂ emissions compared to the combustion of methane.
- The emission of NO_x when hydrogen is added to the fuel increases at the same adiabatic temperature of the flame, which indicates different mechanisms for the formation of nitrogen oxides during the combustion of methane and methane–hydrogen mixtures. However, nitrogen oxide emissions can be achieved by lowering the combustion temperature.
- An increase in the concentration of hydrogen in the mixtures with methane and natural gas is accompanied by an increase in resistance to flame blowout but increases the tendency of the mixture to flashback [58].
- The change in the amplitude of pulsations with increased concentration of hydrogen in the fuel is determined by the initial mechanism of their formation. In this case, the pulsation frequency usually increases.
- As a rule, the effect of increased pressure is more pronounced for the hydrogen–air flame than for the methane–air flame, which complicates the process of interpolating the data obtained under atmospheric conditions for the engine parameters. Thus, further research into the influence of pressure on the combustion of hydrogen presents a crucial task.

Author Contributions: Supervision, E.A.S.; Writing—original draft, I.A.Z., A.Y.K. and M.H.M.; Writing—review & editing, D.V.A., P.A.S., A.G.U. and V.A.D.; Visualization, K.D.T. and D.V.Y. All authors have read and agreed to the published version of the manuscript.

Funding: The work was supported by project FSSS-2022-0019, implemented within the framework of the federal project “Development of human capital in the interests of regions, industries and the research and development sector”, and consequently “New laboratories were created, including those under the guidance of young promising researchers”.

Informed Consent Statement: Informed consent was obtained from all subjects involved in the study.

Conflicts of Interest: The authors declare no conflict of interest.

References

1. Russian Government. Available online: <http://government.ru/docs/42971/> (accessed on 6 March 2023).
2. Acar, C.; Dincer, I. The potential role of hydrogen as a sustainable transportation fuel to combat global warming. *Int. J. Hydrogen Energy* **2020**, *45*, 3396–3406. [\[CrossRef\]](#)
3. Taamallah, S.; Vogiatzaki, K.; Alzahrani, F.M.; Mokheimer, E.M.A.; Habib, M.A.; Ghoniem, A.F. Fuel flexibility, stability and emissions in premixed hydrogen-rich gas turbine combustion: Technology, fundamentals, and numerical simulations. *Appl. Energy* **2015**, *154*, 1020–1047. [\[CrossRef\]](#)
4. Griebel, P. Gas Turbines and Hydrogen. *Hydrog. Sci. Eng. Mater. Process. Syst. Technol.* **2016**, *2*, 1011–1032.
5. Biryuk, V.; Lukachev, S.; Uglanov, D.; Tsybizov, Y. *Gas in Engines*, 1st ed.; Publishing House of Samara University: Samara, Russia, 2021; pp. 3–296.
6. Wallner, T.; Ng, H.K.; Peters, R.W. The effects of blending hydrogen with methane on engine operation, efficiency, and emissions. *SAE Tech. Pap.* **2007**, *2007*, 0474.
7. Wei, J. Boiling points and melting points of chlorofluorocarbons. *Ind. Eng. Chem. Res.* **2000**, *39*, 3116–3119. [\[CrossRef\]](#)
8. GRI-Mech 3.0. Available online: <http://combustion.berkeley.edu/gri-mech/version30/text30.html> (accessed on 6 March 2023).
9. Boushaki, T.; Dhué, Y.; Selle, L.; Ferret, B.; Poinot, T. Effects of hydrogen and steam addition on laminar burning velocity of methane-air premixed flame: Experimental and numerical analysis. *Int. J. Hydrogen Energy* **2012**, *37*, 9412–9422. [\[CrossRef\]](#)
10. Sun, Y.; Zhang, Y.; Huang, M.; Li, Q.; Wang, W.; Zhao, D.; Cheng, S.; Deng, H.; Du, J.; Song, Y.; et al. Effect of hydrogen addition on the combustion and emission characteristics of methane under gas turbine relevant operating condition. *Fuel* **2022**, *324*, 124707. [\[CrossRef\]](#)
11. Li, Z.; Cheng, X.; Wei, W.; Qiu, L.; Wu, H. Effects of hydrogen addition on laminar flame speeds of methane, ethane and propane: Experimental and numerical analysis. *Int. J. Hydrogen Energy* **2017**, *42*, 24055–24066. [\[CrossRef\]](#)
12. Ilbas, M.; Crayford, A.P.; Yilmaz, I.; Bowen, P.J.; Syred, N. Laminar-burning velocities of hydrogen-air and hydrogen-methane-air mixtures: An experimental study. *Int. J. Hydrogen Energy* **2006**, *31*, 1768–1779. [\[CrossRef\]](#)
13. Herzler, J.; Naumann, C. Shock-tube study of the ignition of methane/ethane/hydrogen mixtures with hydrogen contents from 0% to 100% at different pressures. *Proc. Combust. Inst.* **2009**, *32*, 212–220. [\[CrossRef\]](#)
14. Lieuwen, T.; McDonell, V.; Petersen, E.; Santavica, D. Fuel flexibility influences on premixed combustor blowout, flashback, autoignition, and stability. *J. Eng. Gas Turbines Power* **2008**, *130*, 011506. [\[CrossRef\]](#)
15. Beerer, D.J. Autoignition of Methane, Ethane, Propane and Hydrogen in Turbulent High Pressure and Temperature Flows. Master’s Thesis, The University of California, Irvine, CA, USA, 2009.
16. Electronic Fond. Explosionprotected Electrical Apparatus. Part 4. Method of Test for Ignition Temperature. Available online: <https://docs.cntd.ru/document/1200103115?ysclid=lbeo3uxkcl682084142> (accessed on 6 March 2023).
17. Zhang, Y.; Huang, Z. *Experimental and Modeling Study on Auto-Ignition of Methane/hydrogen Blends at Elevated Pressures*; SAE Technical Paper: Warrendale, PA, USA, 2014; p. 1.
18. Gupta, A.; Lilley, D.; Syred, N. *Swirl Flows*, 1st ed.; Abacus Press: Tunbridge Wells, UK, 1984; 488p.
19. Zhang, Y.; Huang, Z.; Wei, L.; Zhang, J.; Law, C.K. Experimental and modeling study on ignition delays of lean mixtures of methane, hydrogen, oxygen, and argon at elevated pressures. *Combust. Flame* **2012**, *159*, 918–931. [\[CrossRef\]](#)
20. Zhang, Y.; Jiang, X.; Wei, L.; Zhang, J.; Tang, C.; Huang, Z. Experimental and modeling study on auto-ignition characteristics of methane/hydrogen blends under engine relevant pressure. *Int. J. Hydrogen Energy* **2012**, *37*, 19168–19176. [\[CrossRef\]](#)
21. Ge, B.; Ji, Y.; Zhang, Z.; Zang, S.; Tian, Y.; Yu, H.; Chen, M.; Jiao, G.; Zhang, D. Experiment study on the combustion performance of hydrogen-enriched natural gas in a DLE burner. *Int. J. Hydrogen Energy* **2019**, *44*, 14023–14031. [\[CrossRef\]](#)
22. Choi, J.; Lee, W.; Rajasegar, R.; Lee, T.; Yoo, J. Effects of hydrogen enhancement on mesoscale burner array flame stability under acoustic perturbations. *Int. J. Hydrogen Energy* **2021**, *46*, 37098–37107. [\[CrossRef\]](#)
23. Chterev, I.; Boxx, I. Effect of hydrogen enrichment on the dynamics of a lean technically premixed elevated pressure flame. *Combust. Flame* **2021**, *225*, 149–159. [\[CrossRef\]](#)
24. Figura, L.; Lee, J.G.; Quay, B.D.; Santavica, D.A. The Effects of Fuel Composition on Flame Structure and Combustion Dynamics in a Lean Premixed Combustor. *ASME* **2007**, *2*, 181–187.
25. Yilmaz, H.; Cam, O.; Yilmaz, I. Experimental investigation of flame instability in a premixed combustor. *Fuel* **2020**, *262*, 116594. [\[CrossRef\]](#)
26. Hu, Z.; Zhang, X. Experimental study on flame stability of biogas / hydrogen combustion. *Int. J. Hydrogen Energy* **2019**, *44*, 5607–5614. [\[CrossRef\]](#)

27. Indlekofer, T.; Ahn, B.; Kwah, Y.H.; Wiseman, S.; Mazur, M.; Dawson, J.R.; Worth, N.A. The effect of hydrogen addition on the amplitude and harmonic response of azimuthal instabilities in a pressurized annular combustor. *Combust. Flame* **2021**, *228*, 375–387. [\[CrossRef\]](#)
28. Wicksall, D.M.; Agrawal, A.K. Acoustics measurements in a lean premixed combustor operated on hydrogen/hydrocarbon fuel mixtures. *Int. J. Hydrogen Energy* **2007**, *32*, 1103–1112. [\[CrossRef\]](#)
29. Kashir, B.; Tabejamaat, S. A numerical study on the effects of H₂ addition in non-premixed turbulent combustion of C₃H₈-H₂-N₂ mixture using a steady flamelet approach. *Int. J. Hydrogen Energy* **2013**, *38*, 9918–9927. [\[CrossRef\]](#)
30. Araoye, A.A.; Abdelhafez, A.; Nemitallah, M.A.; Habib, M.A.; Ben-Mansour, R. Experimental and numerical investigation of stability and emissions of hydrogen-assisted oxy-methane flames in a multi-hole model gas-turbine burner. *Int. J. Hydrogen Energy* **2021**, *46*, 20093–20106. [\[CrossRef\]](#)
31. Bongartz, D.; Ghoniem, A.F. Chemical kinetics mechanism for oxy-fuel combustion of mixtures of hydrogen sulfide and methane. *Combust. Flame* **2015**, *162*, 544–553. [\[CrossRef\]](#)
32. Zhang, P.; Zsély, I.G.; Papp, M.; Nagy, T.; Turányi, T. Comparison of methane combustion mechanisms using laminar burning velocity measurements. *Combust. Flame* **2022**, *238*, 111867. [\[CrossRef\]](#)
33. Verma, S.; Monnier, F.; Lipatnikov, A.N. Validation of leading point concept in RANS simulations of highly turbulent lean syngas-air flames with well-pronounced diffusional-thermal effects. *Int. J. Hydrogen Energy* **2021**, *46*, 9222–9233. [\[CrossRef\]](#)
34. Nemitallah, M.A.; Imteyaz, B.; Abdelhafez, A.; Habib, M.A. Experimental and computational study on stability characteristics of hydrogen-enriched oxy-methane premixed flames. *Appl. Energy* **2019**, *250*, 433–443. [\[CrossRef\]](#)
35. Bouras, F.; El Hadi Attia, M.; Khaldi, F.; Si-Ameur, M. Control of methane flame properties by hydrogen fuel addition: Application to power plant combustion chamber. *Int. J. Hydrogen Energy* **2017**, *42*, 8932–8939. [\[CrossRef\]](#)
36. Kim, H.S.; Arghode, V.K.; Gupta, A.K. Flame characteristics of hydrogen-enriched methane-air premixed swirling flames. *Int. J. Hydrogen Energy* **2009**, *34*, 1063–1073. [\[CrossRef\]](#)
37. Rahimi, S.; Mazaheri, K.; Alipoor, A.; Mohammadpour, A. The effect of hydrogen addition on methane-air flame in a stratified swirl burner. *Energy* **2023**, *265*, 126354. [\[CrossRef\]](#)
38. Kim, H.S.; Arghode, V.K.; Linck, M.B.; Gupta, A.K. Hydrogen addition effects in a confined swirl-stabilized methane-air flame. *Int. J. Hydrogen Energy* **2009**, *34*, 1054–1062. [\[CrossRef\]](#)
39. Leng, X.; Huang, H.; Ge, Q.; He, Z.; Zhang, Y.; Wang, Q.; He, D.; Long, W. Effects of hydrogen enrichment on the combustion and emission characteristics of a turbulent jet ignited medium speed natural gas engine: A numerical study. *Fuel* **2021**, *290*, 119966. [\[CrossRef\]](#)
40. Abubakar, Z.; Shakeel, M.R.; Mokheimer, E.M.A. Experimental and numerical analysis of non-premixed oxy-combustion of hydrogen-enriched propane in a swirl stabilized combustor. *Energy* **2018**, *165*, 1401–1414. [\[CrossRef\]](#)
41. Therkelsen, P.; Werts, T.; McDonell, V.; Samuelsen, S. Analysis of NO_x Formation in a Hydrogen-Fueled Gas Turbine Engine. *ASME* **2009**, *131*, 031507. [\[CrossRef\]](#)
42. Hashemi, S.A.; Hajjaligol, N.; Mazaheri, K.; Fattahi, A. Investigation of the effect of the flame holder geometry on the flame structure in non-premixed hydrogen-hydrocarbon composite fuel combustion. *Combust. Explos. Shock. Waves* **2014**, *50*, 32–41. [\[CrossRef\]](#)
43. Ghoniem, A.F.; Annaswamy, A.; Park, S.; Sobhani, Z.C. Stability and emissions control using air injection and H₂ addition in premixed combustion. *Proc. Combust. Inst.* **2005**, *30*, 1765–1773. [\[CrossRef\]](#)
44. Chen, Z.; Yong, J. Numerical investigation of the effects of H₂/CO/syngas additions on laminar premixed combustion characteristics of NH₃/air flame. *Int. J. Hydrogen Energy* **2021**, *46*, 12016–12030. [\[CrossRef\]](#)
45. Kim, N.; Kim, V.; Jaafar, M.N.M.; Rahim, M.R.; Said, M. Effects of hydrogen addition on structure and NO formation of highly CO-Rich syngas counterflow nonpremixed flames under MILD combustion regime. *Int. J. Hydrogen Energy* **2021**, *46*, 10518–10534. [\[CrossRef\]](#)
46. Semenikhin, A.S.; Matveev, S.S.; Chechet, I.V.; Matveev, S.G.; Idrisov, D.V.; Gurakov, N.I.; Radin, D.V.; Novichkova, S.S.; Fokin, N.I.; Simin, N.O.; et al. Kinetic Models of Methane-Hydrogen Mixture Combustion: Brief Review and Validation. *Therm. Eng.* **2022**, *69*, 792–801. [\[CrossRef\]](#)
47. Papanikolaou, N.; Wierzbna, I. The effects of burner geometry and fuel composition on the stability of a jet diffusion flame. *J. Energy Resour. Technol. Trans. ASME* **1997**, *119*, 265–270. [\[CrossRef\]](#)
48. Karbasi, M.; Wierzbna, I. The effects of hydrogen addition on the stability limits of methane jet diffusion flames. *Int. J. Hydrogen Energy* **1998**, *23*, 123–129. [\[CrossRef\]](#)
49. Schefer, R.W.; Wicksall, D.M.; Agrawal, A.K. Combustion of hydrogen-enriched methane in a lean premixed swirl-stabilized burner. *Proc. Combust. Inst.* **2002**, *29*, 843–851. [\[CrossRef\]](#)
50. Zhu, S.; Acharya, S. An experimental study of lean blowout with hydrogen-enriched fuels. *J. Eng. Gas Turbines Power* **2012**, *134*, 041507. [\[CrossRef\]](#)
51. Schefer, R.W. Hydrogen enrichment for improved lean flame stability. *Int. J. Hydrogen Energy* **2003**, *28*, 1131–1141. [\[CrossRef\]](#)
52. Griebel, P.; Boschek, E.; Jansohn, P. Lean Blowout Limits and NO_x Emissions of Turbulent, Lean Premixed, Hydrogen-Enriched Methane/Air Flames at High Pressure. *ASME* **2006**, *1*, 405–412.
53. Choi, J.; Rajasegar, R.; Lee, W.; Lee, T.; Yoo, J. Hydrogen enhancement on a mesoscale swirl stabilized burner array. *Int. J. Hydrogen Energy* **2021**, *46*, 23906–23915. [\[CrossRef\]](#)

54. Zhang, J.; Ratner, A. Experimental study of the effects of hydrogen addition on the thermoacoustic instability in a variable-length combustor. *Int. J. Hydrogen Energy* **2021**, *46*, 16086–16100. [[CrossRef](#)]
55. Davis, D.W.; Therkelsen, P.L.; Littlejohn, D.; Cheng, R.K. Effects of hydrogen on the thermo-acoustics coupling mechanisms of low-swirl injector flames in a model gas turbine combustor. *Proc. Combust. Inst.* **2013**, *34*, 3135–3143. [[CrossRef](#)]
56. Shanbhogue, S.J.; Sanusi, Y.S.; Taamallah, S.; Habib, M.A.; Mokheimer, E.M.A.; Ghoniem, A.F. Flame macrostructures, combustion instability and extinction strain scaling in swirl-stabilized premixed CH₄/H₂ combustion. *Combust. Flame* **2016**, *167*, 497. [[CrossRef](#)]
57. Zhang, J.; Ratner, A. Experimental study on the excitation of thermoacoustic instability of hydrogen-methane/air premixed flames under atmospheric and elevated pressure conditions. *Int. J. Hydrogen Energy* **2019**, *44*, 21324–21335. [[CrossRef](#)]
58. Yilmaz, I.; Ratner, A.; Ilbas, M.; Huang, Y. Experimental investigation of thermoacoustic coupling using blended hydrogen-methane fuels in a low swirl burner. *Int. J. Hydrogen Energy* **2010**, *35*, 329–336. [[CrossRef](#)]
59. El-Ghafour, S.A.A.; El-dein, A.H.E.; Aref, A.A.R. Combustion characteristics of natural gas-hydrogen hybrid fuel turbulent diffusion flame. *Int. J. Hydrogen Energy* **2010**, *35*, 2556–2565. [[CrossRef](#)]
60. Imteyaz, B.A.; Nemitallah, M.A.; Abdelhafez, A.A.; Habib, M.A. Combustion behavior and stability map of hydrogen-enriched oxy-methane premixed flames in a model gas turbine combustor. *Int. J. Hydrogen Energy* **2018**, *43*, 16652–16666. [[CrossRef](#)]
61. Zhang, W.; Wang, J.; Lin, W.; Mao, R.; Xia, H.; Zhang, M.; Huang, Z. Effect of differential diffusion on turbulent lean premixed hydrogen enriched flames through structure analysis. *Int. J. Hydrogen Energy* **2020**, *45*, 10920–10931. [[CrossRef](#)]
62. Lee, T.W.; North, G.L.; Santavica, D.A. Surface properties of turbulent premixed propane/air flames at various Lewis numbers. *Combust. Flame* **1993**, *93*, 445–456. [[CrossRef](#)]
63. Aspden, A.J.; Day, M.S.; Bell, J.B. Lewis number effects in distributed flames. *Proc. Combust. Inst.* **2011**, *33*, 1473–1480. [[CrossRef](#)]
64. Burbano, H.J.; Pareja, J.; Amell, A.A. Laminar burning velocities and flame stability analysis of H₂/CO/air mixtures with dilution of N₂ and CO₂. *Int. J. Hydrogen Energy* **2011**, *36*, 3232–3242. [[CrossRef](#)]
65. Dinkelacker, F.; Manickam, B.; Muppala, S.P.R. Modelling and simulation of lean premixed turbulent methane/hydrogen/air flames with an effective Lewis number approach. *Combust. Flame* **2011**, *158*, 1742–1749. [[CrossRef](#)]
66. Bell, J.B.; Cheng, R.K.; Day, M.S.; Shepherd, I.G. Numerical simulation of Lewis number effects on lean premixed turbulent flames. *Proc. Combust. Inst.* **2007**, *31*, 1309–1317. [[CrossRef](#)]
67. Lee, H.C.; Dai, P.; Wan, M.; Lipatnikov, A.N. Lewis number and preferential diffusion effects in lean hydrogen–air highly turbulent flames. *Phys. Fluids* **2022**, *34*, 035131. [[CrossRef](#)]
68. Aspden, A.J.; Bell, J.B.; Woosley, S.E.; Zingale, M. Turbulence-Flame Interactions in Type Ia Supernovae. *Astrophys. J.* **2008**, *2*, 1173–1185. [[CrossRef](#)]

Disclaimer/Publisher’s Note: The statements, opinions and data contained in all publications are solely those of the individual author(s) and contributor(s) and not of MDPI and/or the editor(s). MDPI and/or the editor(s) disclaim responsibility for any injury to people or property resulting from any ideas, methods, instructions or products referred to in the content.